

A SINGLE-FIELD SWAT MODEL APPROACH TO EVALUATE IMPROVEMENTS IN  
PROCESS REPRESENTATION FOR PERCHED WATER TABLE DEPTH SIMULATION  
AND SOIL TEMPERATURE DYNAMICS

by

Jaya L. Hafner

A thesis submitted in partial fulfillment of  
the requirements for the degree of

Master of Science

(Agroecology)

at the

UNIVERSITY OF WISCONSIN-MADISON

2025

## Table of Contents

List of Tables.....	iii
List of Figures.....	iv
Acknowledgements.....	vi
Abstract.....	vii
1. Introduction.....	1
1.1. Importance of model improvements to soil temperature.....	4
1.2. Importance of model improvements to perched water table simulation.....	5
1.3. Thesis objectives.....	6
2. Methods.....	7
2.1. Development of a single field model.....	7
2.1.1. Study area.....	7
2.1.2. Available data from the study site.....	8
2.1.3. SWAT model input data.....	9
2.2. Improvements to soil temperature simulation in the SWAT source code.....	16
2.3. Improvements to the perched water table algorithm in the SWAT source code.....	17
2.3.1. Revised Modified DRAINMOD Approach.....	18
2.3.2. Kalcic Lab improvements to perched water table depth calculation.....	21
2.3.3. Tile flow calculation.....	25
2.4. Model calibration and validation.....	26
2.4.1. Using SWATrunR for model calibration.....	30
2.4.2. Model evaluation.....	31
3. Results.....	32
3.1. Evaluating soil temperature improvements made by Qi et al. (2016a,b; 2019).....	33
3.2. Evaluating improvements to the perched water table algorithm.....	38
3.3. Evaluating improvements to the perched water table algorithm without SWAT-FT.....	44
3.4. Cold season results.....	50
4. Discussion and future work.....	52
4.1. The single field model.....	52
4.2. Soil temperature outputs.....	52
4.3. Hydrology outputs.....	54
4.4. Calibration.....	56
5. Conclusion.....	58
References.....	59
Appendices.....	69

## List of Tables

<b>Table 1:</b> In-field and edge-of-field monitoring data used to calibrate and validate the SWAT model .....	8
<b>Table 2:</b> Management input data for study field 2016-2023. The period 2013-2015 was assumed to have identical management to 2019-2021 .....	9
<b>Table 3:</b> SWAT model inputs and settings .....	10
<b>Table 4:</b> SWAT parameters, the initial and final values, the reason for the value change, and a description of the value. Complete .sol and .chm values can be found in the Appendix (6-7) .....	12
<b>Table 5:</b> Description of parameters for calibration, original values, calibration ranges, reasoning for selecting the range, and a description of the parameter being used .....	28
<b>Table 6:</b> Calibration and validation periods for each model output .....	30
<b>Table 7:</b> Model calibration results for 15 SWAT parameters .....	32
<b>Table 8:</b> RSR scores comparing eight SWAT outputs across two executables. The two executables compared are (1) the <i>IWTDN=1</i> & <i>SWAT-FT</i> executable (represented by the dark blue line in figures 8-11) and (2) the <i>IWTDN=1</i> executable (represented by the light blue line in figures 8-11). Moriasi et al. (2007b) indicates that 0.7 and less is a satisfactory RSR at the watershed scale in a monthly time interval. Moriasi (2007) considers a RSR of 0.5 and less to be very good. Satisfactory values are in bold .....	34
<b>Table 9:</b> RSR scores comparing eight SWAT outputs across two executables. The two executables compared are (1) the <i>IWTDN=2</i> & <i>SWAT-FT</i> executable (represented by the red line in figures 12-16) and (2) the <i>IWTDN=1</i> & <i>SWAT-FT</i> executable (represented by the dark blue line in figures 12-16). Moriasi et al. (2007b) indicates that 0.7 and less is a satisfactory RSR at the watershed scale in a monthly time interval. Satisfactory values are in bold .....	39
<b>Table 10:</b> RSR scores standardized by standard deviation comparing eight SWAT outputs across two executables. The two executables compared are (1) the <i>IWTDN=1</i> executable (represented by the light blue line in figures 17-20) and (2) the <i>IWTDN=2</i> executable (represented by the green line in figures 17-20). Moriasi et al. (2007b) indicates that 0.7 and less is a satisfactory RSR at the watershed scale in a monthly time interval. Satisfactory values are in bold .....	45
<b>Table 11:</b> RSR statistics for only the cold seasons (12/1-3/31) during the calibration period for each executable (Table 6). The model was not calibrated to these metrics. Moriasi et al. (2007b) indicates that 0.7 and less is a satisfactory RSR at the watershed scale in a monthly time interval. Satisfactory values are in bold .....	50
<b>Table 12:</b> RSR statistics for only the cold seasons (12/1-3/31) during the validation period for each executable (Table 6). Moriasi et al. (2007b) indicates that 0.7 and less is a satisfactory RSR at the watershed scale in a monthly time interval. Satisfactory values are in bold .....	51

## List of Figures

<b>Figure 1:</b> Map of the single-field SWAT model in Hardin County, Ohio (ESRI Census 2000 TIGER county layer and ArcGIS Pro basemap) .....	7
<b>Figure 2:</b> Precipitation over the period of time that there is measured data (2020-2023) .....	11
<b>Figure 3:</b> Minimum and maximum air temperature over the period of time that there is measured data (2020-2023) .....	11
<b>Figure 4:</b> A representation of the soil temperature algorithm before and after the addition of Qi's physically-based equation for one-dimensional heat transfer (Neitsch et al., 2009; Qi et al., 2016a) .....	17
<b>Figure 5:</b> Example of the perched water table calculations in the Revised modified DRAINMOD approach .....	20
<b>Figure 6:</b> Example of the perched water table calculations in the Kalcic Lab approach .....	24
<b>Figure 7:</b> The four SWAT executables tested in this thesis .....	26
<b>Figure 8:</b> Time series of soil temperature (°C) at 100 mm, 200 mm, and 500 mm from June 2020 through the end of 2023. Measured data is represented by the black line, the <i>IWTDN=1</i> & <i>SWAT-FT</i> output is represented by the dark blue line, and the <i>IWTDN=1</i> output is represented by the light blue line. The validation period (ends 09/30/2021) is separated from the calibration period (starts 10/01/2021) by the vertical dashed line. Cold seasons (12/1-3/31) are highlighted in grey .....	35
<b>Figure 9:</b> Time series of flow through the tile drains (mm) from January 2020 through the end of 2023. Measured data is represented by the black line, the <i>IWTDN=1</i> & <i>SWAT-FT</i> output is represented by the dark blue line, and the <i>IWTDN=1</i> output is represented by the light blue line. The validation period (ends 09/30/2021) is separated from the calibration period (starts 10/01/2021) by the vertical dashed line. Cold seasons (12/1-3/31) are highlighted in grey .....	36
<b>Figure 10:</b> Time series of perched water table depth from the soil surface (mm) from May 2022 through the end of 2023. Measured data is represented by the black line, the <i>IWTDN=1</i> & <i>SWAT-FT</i> output is represented by the dark blue line, and the <i>IWTDN=1</i> output is represented by the light blue line. Cold seasons (12/1-3/31) are highlighted in grey .....	37
<b>Figure 11:</b> Time series of soil volumetric water content at 100 mm, 200 mm, and 500 mm from June 2020 through the end of 2023 in mm/mm. Measured data is represented by the black line, the <i>IWTDN=1</i> & <i>SWAT-FT</i> output is represented by the dark blue line, and the <i>IWTDN=1</i> output is represented by the light blue line. The validation period (ends 09/30/2021) is separated from the calibration period (starts 10/01/2021) by the vertical dashed line. Cold seasons (12/1-3/31) are highlighted in grey .....	38
<b>Figure 12:</b> Time series of soil temperature (°C) at 100 mm, 200 mm, and 500 mm from June 2020 through the end of 2023. Measured data is represented by the black line, the <i>IWTDN=2</i> & <i>SWAT-FT</i> executable is represented by the red line, and the <i>IWTDN=1</i> & <i>SWAT-FT</i> executable is represented by the dark blue line. The validation period (ends 09/30/2021) is separated from the calibration period (starts 10/01/2021) by the vertical dashed line. Cold seasons (12/1-3/31) are highlighted in grey .....	40
<b>Figure 13:</b> Time series of flow through the tile drains (mm) from January 2020 through the end of 2023. Measured data is represented by the black line, the <i>IWTDN=2</i> & <i>SWAT-FT</i> executable is represented by the red line, and the <i>IWTDN=1</i> & <i>SWAT-FT</i> executable is represented by the dark blue line. The	

validation period (ends 09/30/2021) is separated from the calibration period (starts 10/01/2021) by the vertical dashed line. Cold seasons (12/1-3/31) are highlighted in grey .....41

**Figure 14:** Time series of perched water table depth from the soil surface (mm) from May 2022 through the end of 2023. Measured data is represented by the black line, the *IWTDN=2 & SWAT-FT* executable is represented by the red line, and the *IWTDN=1 & SWAT-FT* executable is represented by the dark blue line. Cold seasons (12/1-3/31) are highlighted in grey .....42

**Figure 15:** Time series of soil volumetric water content at 100 mm, 200 mm, and 500 mm from June 2020 through the end of 2023 in mm/mm. Measured data is represented by the black line, the *IWTDN=2 & SWAT-FT* executable is represented by the red line, and the *IWTDN=1 & SWAT-FT* executable is represented by the dark blue line. The validation period (ends 09/30/2021) is separated from the calibration period (starts 10/01/2021) by the vertical dashed line. Cold seasons (12/1-3/31) are highlighted in grey .....43

**Figure 16:** Time series of flow through the tile drains (mm), precipitation (mm), and perched water table depth (mm) during the calibration period. Measured data is represented by the black line, the SWAT output using the *IWTDN=2 & SWAT-FT* executable is represented by the red line, and the SWAT output from the *IWTDN=1 & SWAT-FT* executable is represented by the dark blue line. Cold seasons (12/1-3/31) are highlighted in grey .....44

**Figure 17:** Time series of soil temperature (°C) at 100 mm, 200 mm, and 500 mm from June 2020 through the end of 2023. Measured data is represented by the black line, the *IWTDN=1* executable is represented by the light blue line, and the *IWTDN=2* executable is represented by the green line. The validation period (ends 09/30/2021) is separated from the calibration period (starts 10/01/2021) by the vertical dashed line. Cold seasons (12/1-3/31) are highlighted in grey .....46

**Figure 18:** Time series of flow through the tile drains (mm) from January 2020 through the end of 2023. Measured data is represented by the black line, the *IWTDN=1* executable is represented by the light blue line, and the *IWTDN=2* executable is represented by the green line. The validation period (ends 09/30/2021) is separated from the calibration period (starts 10/01/2021) by the vertical dashed line. Cold seasons (12/1-3/31) are highlighted in grey .....47

**Figure 19:** Time series of perched water table depth from the soil surface (mm) from May 2022 through the end of 2023. Measured data is represented by the black line, the *IWTDN=1* executable is represented by the light blue line, and the *IWTDN=2* executable is represented by the green line. The validation period (ends 09/30/2021) is separated from the calibration period (starts 10/01/2021) by the vertical dashed line. Cold seasons (12/1-3/31) are highlighted in grey .....48

**Figure 20:** Time series of soil volumetric water content at 100 mm, 200 mm, and 500 mm from June 2020 through the end of 2023 in mm/mm. Measured data is represented by the black line, the *IWTDN=1* executable is represented by the light blue line, and the *IWTDN=2* executable is represented by the green line. The validation period (ends 09/30/2021) is separated from the calibration period (starts 10/01/2021) by the vertical dashed line. Cold seasons (12/1-3/31) are highlighted in grey .....49

## Acknowledgements

I am deeply grateful for the mentorship and support of my PI, Dr. Margaret Kalcic. Her patience, encouragement, and kindness are greatly appreciated. She is a wonderful teacher, and I have learned an incredible amount during my time as her student. Thank you as well to Dr. Anita Thompson and Dr. Laxmi Prasad, my committee members, for the time, thoughtful guidance, and expertise they have shared throughout my master's program.

I would also like to sincerely thank Dr. Lourdes Arrueta Antequera for her help with source code modification, insights into SWAT processes, and steady guidance. Her contributions have been instrumental, and I am truly grateful for her mentorship. Thank you to the broader Thompson-Kalcic-Nocco-Arriaga Lab group for their support, camaraderie, and helpful feedback during this degree. I am also grateful for the Agroecology program and its students for its encouragement and interdisciplinary perspective.

I am grateful to the USDA-ARS for the field data that made this project possible. Thank you to the USDA NIFA program for the funding that enabled this project. My appreciation also goes to the NIFA-Frozen and NIFA-Tile P groups for their helpful feedback, problem-solving, and continued support.

Lastly, a heartfelt thank you to my wonderful family and friends. To my parents who have encouraged me in every way imaginable and attended every performance and presentation since I was little. To my brother, who has always cheered me on. And to my husband, Tav, thank you for being there to help with late night coding problems, for supporting me always, and for moving to Madison so I could follow my dreams and complete my master's.

## Abstract

While the Midwest has fertile soil ideal for agricultural production, in many cases these soils were historically wetlands that have been artificially drained. A soil profile with a seasonally high perched water table is not suitable for growing most crops. Subsurface (“tile”) drainage helps lower the soil water table and increase crop yield by moving water out of the farm field through subsurface waterways. However, tile drains are also a direct conduit for nutrients to leave the field. Nutrient runoff contributes to harmful algal blooms and dead zones, which threaten ecosystems and human health. The Soil and Water Assessment Tool (SWAT) is a hydrologic model used to simulate the effects of land use, topography, soil type, and climate on hydrology and nutrient runoff. Several states rely on SWAT to calculate total maximum daily loads (TMDLs) and guide progress toward water quality goals. However, previous studies have identified areas for improvement in SWAT’s ability to simulate cold-season processes. Research has also indicated that the calculation of the perched water table depth is not fully tied to soil moisture by layer or tile flow. To address this, (1) a single-field SWAT model was developed, (2) a physically based soil temperature equation created by Qi et al. (2016a,b; 2019) was integrated into the SWAT source code, (3) a new method of calculating perched water table depth by using soil water by layer above field capacity was added to the SWAT source code, and (4) the single-field SWAT model was calibrated to evaluate model improvements. Improvements to soil temperature simulation by Qi et al. (2016a,b; 2019) were found to improve both soil temperature simulation ( $RSR < 0.5$ ) and some subsurface hydrology parameters when compared to measured data. Statistical results for the perched water table improvements to the SWAT source code were mixed for hydrologic variable outputs. However, this thesis is the first step in improving the simulation of the perched water table, and further improvements are needed.

## 1. Introduction

While the Midwest has fertile soil ideal for agricultural production, in many cases these soils were historically wetlands that have been artificially drained. It is estimated that the Midwest corn belt (Illinois, Indiana, Iowa, Michigan, Minnesota, Ohio, and Wisconsin) has lost 36 million acres of wetlands since the late 1700's (Dahl, 1990). Agricultural yields depend on the perfect balance of soil water. A soil profile with a seasonally high perched water table can create an anoxic environment around the plant roots, generate excessive surface runoff, and lead to increased soil erosion (Darzi-Naftchali et al., 2013; Skaggs et al., 1994). The solution to poorly draining soil for Midwest agriculture was subsurface ("tile") drainage. Tile drains move water out of the farm field through subsurface waterways helping lower the soil water table, reducing soil salinity, preventing erosion, and minimizing surface runoff (Shedekar et al., 2020). Today, tile drainage is an important component of subsurface hydrology for agricultural production across the country, but it is especially prevalent in the Midwest where 83.8% of tile drains in the United States are located (Valayamkunnath et al., 2020).

Subsurface drainage for agriculture was first implemented in the United States in 1838 using clay tiles to build underground drainage pathways (Shedekar et al., 2020). After World War II, developments in agricultural machinery allowed farms to increase in size, and the need for more complex subsurface drainage also increased (Madramootoo et al., 2007). Corrugated plastic tubing was developed in the 1960's which lowered the cost of tile drain implementation and increased tile drain usage (Fouss, 1973). The addition of tile drainage to agricultural fields has increased crop yield across the North-Central region of the United States (Mourtzinis et al., 2021).

While tile drains are able to increase crop yield, they also create a fast track for nutrients to leave the field and enter nearby streams and waterways (King et al., 2014). Nitrogen and phosphorus are key nutrients for plant growth and are applied to farm fields across the United States. Nutrients from fertilization are lost from the field through many mediums, including through tile drains (Duncan et al., 2017; Hanrahan et

al., 2019; Osterholz et al., 2020). There are ways to reduce nitrogen and phosphorus nutrient loss from tile drains through farm management techniques such as implementing crop rotations, soil testing, reduced fertilizer application, fertilizer application timing, subsurface fertilizer application, and cover cropping (King et al., 2018; Kladivko et al., 2004; 2021).

In the Midwest corn belt, nutrient runoff has generated water quality problems in the Great Lakes Basin that have led to ecosystem degradation, economic concerns, and human health problems (Dodds et al., 2009). Over 30% of the land around the Great Lakes Basin is farm land (Kerr et al., 2016). Lake Erie is a particularly shallow Great Lake, and also has the largest amount of surrounding agricultural land in the watershed (Stewart, 2013). Increased nitrogen and phosphorus loading into Lake Erie due to farming practices has been tied to increased frequency of harmful algal blooms (Chaffin et al., 2018; Michalack et al., 2013; OLEPT Force, 2013; Paerl et al., 2016). More frequent harmful algal blooms have led to an increase in legislation and industry stewardship reform in an attempt to reduce runoff in the area (Vollmer-Sanders et al., 2016). The effort to reduce nutrient inputs into the Great Lake Basin, and Lake Erie in particular, underscores the importance of understanding the biogeochemical processes contributing to nutrient loss in the region.

Within the Western Lake Erie Basin (WLEB), soils have a high clay percentage and are relatively flat, which requires the use of tile drains (Jaynes and James, 2007; Williams et al., 2016). The Western Lake Erie Basin has one of the largest concentrations of tile drains in the country, with 60% of cropland having tiles (Jaynes and James, 2007; OLEPTF, 2013). One study in the WLEB saw fields lose 49% of phosphorus through tile drains (Smith et al., 2015). Another study in Ohio found 62% of nitrate-nitrogen was lost through tiles (Williams et al., 2015). These findings highlight the importance of understanding and predicting subsurface hydrology in the WLEB, as the number and intensity of tile drained fields continue to increase.

In the WLEB and greater Midwest region, it is important that policy supports reduction in nutrient runoff from working lands. States across the country, including Ohio, use total maximum daily loads (TMDLs) to provide pollution budgeting guidelines for non-point source pollution, such as agricultural nutrient runoff, and to prevent algal blooms and poor water quality (Nietch et al., 2023). TMDLs are supported by SWAT to provide load duration curves for nutrients (Nietch et al., 2023; The Cadmus Group, 2012). It is important that SWAT is simulating subsurface hydrology accurately in order to inform TMDLs and effectively reduce nutrient runoff.

SWAT was developed by the USDA Agricultural Research Service (USDA-ARS) and Texas A&M AgriLife Research to evaluate the effect of land use on water resources (Arnold et al., 1998). SWAT uses adjustable, physically-based parameters, as well as soil properties, land use characteristics, elevation, and climate data, to calculate the hydrology and movement of nutrients across the landscape. SWAT's ability to evaluate land use and climate regime impacts on water resources in areas with no measured data as well as its ability to predict future trends have led to wide usage by regulatory agencies and the scientific community (Neitsch et al., 2009). There are many different versions of SWAT: SWAT2000, SWAT2005, SWAT2009, SWAT2012, and SWAT+ (SWAT Documentation, n.d.). This thesis will employ SWAT2012 because source code improvements used in this project were created for SWAT2012 (Qi et al., 2016a) and because of the well documented source code structure (SWAT Documentation, n.d.). SWAT2012 will hereby be referred to as "SWAT".

While SWAT is a trusted model for modeling hydrology and water quality in agroecosystems (Douglas-Mankin et al., 2010), SWAT has certain limitations that prevent it from accurately simulating water and nutrient losses through tile drainage. Limitations of SWAT include first, the simulation of cold region processes, such as freeze-thaw cycles and water movement in frozen and partially frozen soils (Qi et al., 2016a,b; 2019). Second, SWAT also has room for improvement in the simulation of perched water

table depth to make the calculations more fully coupled to moisture in the soil profile above the drains (SWAT2012 ver. 692 as of 11/14/2023).

### 1.1. Importance of model improvements to soil temperature

Studies have shown that SWAT's hydrology and nutrient runoff simulation during the cold season does not match measured data (Li et al., 2014; Yang et al., 2009, 2012). To simulate soil temperature, SWAT uses an empirical model based on the temperature of the soil the day of and the day before, the average air temperature annually, and depth from soil surface (Neitsch et al., 2009). This empirical model does not take into account how hydrology within the soil profile is affected by the phase changes of water or the insulation provided by snow on the soil surface (Qi et al., 2016a,b). A different approach was needed to improve SWAT hydrology outputs during the winter. This thesis integrates improved one-dimensional heat transfer equations from Qi et al. (2016a,b; 2019) for simulating cold-season soil temperature and moisture to improve SWAT's ability to simulate cold-season hydrology. For the purpose of this thesis, the cold season is defined as the beginning of December to the end of March.

Improving the simulation of cold region hydrology in SWAT is important because winter is a critical season for the water cycle and hydrologic dynamics during the freeze-thaw period are critical for understanding nutrient runoff from farms. In livestock-centric production systems, manure is often applied to fields at the end of the growing season in late fall. During winter in cold regions, temperatures drop and working lands lie fallow. Then, the freeze thaw period in early spring carries nutrients applied the previous fall into waterways (Gray and Landine, 1988; Plach et al., 2019).

Nutrient runoff and water quality are closely related to soil properties and structure (Doran et al., 2000). Different soil types, land use, and management practices can contribute to changes in water quality. For example, no-till and reduced till have been advertised as best management practices for improving soil quality. However, properties of frozen soils, such as a smoother texture, can increase snowmelt and

nutrient runoff on farms that practice no-till (Zopp et al., 2019). In fact, there are areas around Lake Erie where no-till has been linked to an increase in phosphorus runoff in the area, whether the farm has tile drainage or not (Bosch et al., 2014; Kleinman et al., 2015). It is impossible to measure runoff from every field in a large region to understand the intricacies of what farming practices would reduce water pollution. Hydrologic models such as SWAT are able to handle large scale analysis and test numerous scenarios across the Midwest.

### 1.2. Importance of model improvements to perched water table simulation

The current SWAT source code (1) uses a water table adjustment factor that was calibrated to a specific region's hydrology and (2) does not fully tie soil moisture by layer to perched water table depth which disconnects the SWAT algorithms from what is happening in reality within the soil profile (SWAT2012 ver. 692 as of 11/14/2023). The disconnect between the SWAT algorithms and soil water allows scenarios where the perched water table is simulated to be high despite low soil moisture and tile flow—a physical impossibility. This thesis proposes a simple approach for perched water table depth calculation based on soil moisture above field capacity by layer, in order to make the water table calculations more physically accurate.

Perched water table depth from the soil surface is also important within the SWAT model because it affects many aspects of agriculture such as soil salinity and subsurface tile flow, which influence crop yield (Kahlow et al., 2005, Wang et al., 2004, Xu et al., 2013). Within the SWAT model, the perched water table in SWAT affects how the model simulates subsurface tile flow (Neitsch et al., 2009; SWAT2012 ver. 692 as of 11/14/2023).

### 1.3. Thesis objectives

This research aims to ultimately improve SWAT model predictions by making the equations used in the SWAT source code more physically based in soil temperature and perched water table calculations. The

goal of the source code improvements is to particularly improve predictions in areas with cold seasons where wintertime runoff is responsible for water quality issues, as well as in regions with subsurface drainage and seasonal high water table. Ultimately, the improved SWAT source code will help stakeholders, such as policy makers and scientists, make more informed farm management decisions to improve water quality.

The goal of this project is to improve the simulation of subsurface hydrology and soil temperature through (1) development of a single-field SWAT model at a heavily-monitored site for rigorous testing of algorithms, (2) incorporation of a cold-season dynamic algorithm developed by Qi et al. (2016a,b; 2019) into SWAT source code version 664, (3) improved simulation of the perched water table to closely couple soil moisture and water table integrated into SWAT source code version 664, and (4) calibration of the single-field SWAT model and evaluation of source code improvements.

## 2. Methods

### 2.1. Development of a single field model

SWAT models are typically built at the watershed scale. However, this SWAT model was created for a single field with a high frequency and duration of in-field and edge-of-field monitoring to serve as a testbed for evaluation of the key algorithm improvements in the source code. Additionally, a field-scale model enables prediction at a field-scale, and it creates an environment where it is easier to see the model's response to source code changes.

#### 2.1.1. Study area

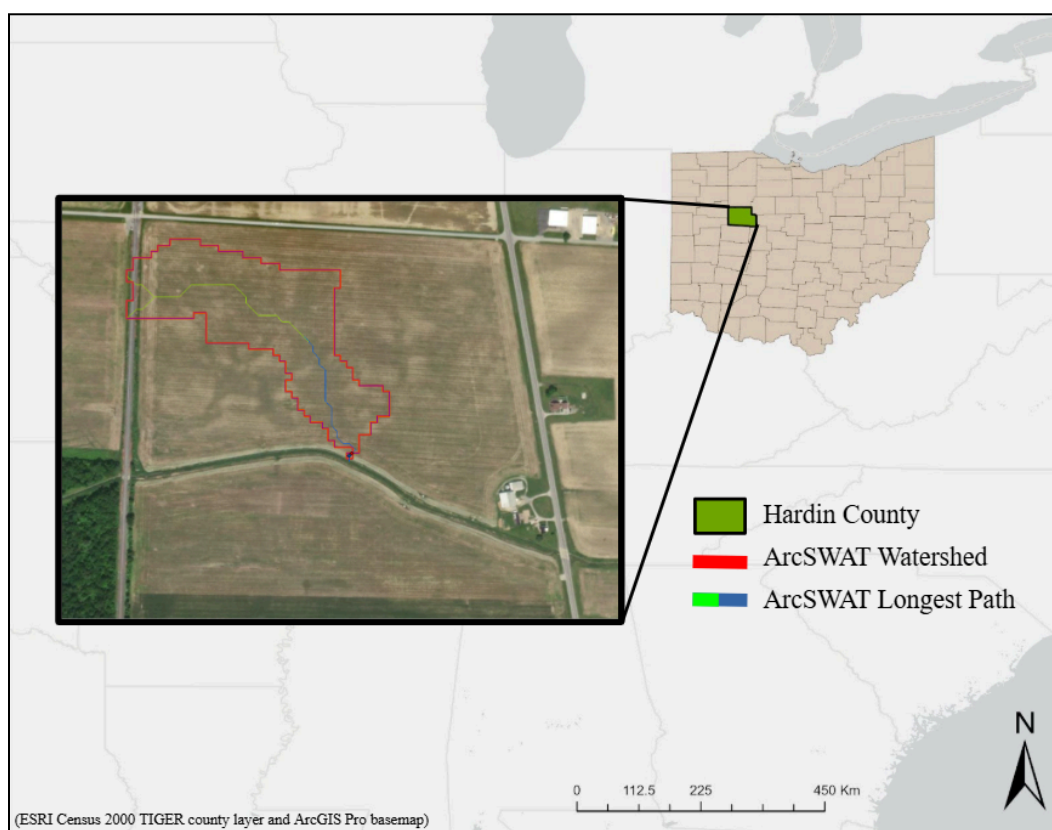


**Figure 1:** Map of the single-field SWAT model in Hardin County, Ohio (ESRI Census 2000 TIGER county layer and ArcGIS Pro basemap).

The SWAT model is set up for a single field in Hardin County, Ohio. The SWAT watershed is  $0.0619 \text{ km}^2$  and is a corn-soy rotation with management data from 2016-2023 (Tables 1-2). The soil is majority

Blount silt loam, a soil formed by glacial till (Morse, 1958). Blount has a high clay content resulting in poor natural drainage that requires tile drainage to make the land suitable for agriculture.

### 2.1.2. Available data from the study site

The USDA-ARS worked with farmers in Ohio to collect the in-field and edge-of-field data that was used to calibrate and validate SWAT model outputs. Model set-up is outlined in Tables 3 and 4.

**Table 1:** In-field and edge-of-field monitoring data used to calibrate and validate the SWAT model.

Data type collected	Time period	Reporting interval	Collection method	Data transformation
Tile flow (mm)	1/1/2020-12/31/2023	Sub-daily	Edge-of-field tile flow measurements were taken every ten minutes by a bubbler flow meter (Teledyne Isco 4230). When the water level was above the tile drains, an area velocity sensor was used (Teledyne Isco 2150) (King et al., 2018; Pease et al., 2018).	Flow summed for a given day
Perched water table depth from soil surface (mm)	5/12/2022-12/31/2023	Sub-daily	Observation wells were installed between the tile laterals and deeper than the invert of the subsurface drainage outlet (>3m). Middle-of-field measurements were taken each hour using Pendant level loggers (Solinst).	Maximum value per day to capture the deepest the water table is from the surface during a given day
Volumetric water content at 100, 200, and 500 mm as a fraction	6/17/2020-12/31/2023	Sub-daily	Volumetric water content (dielectric impedance-based) and soil temperature sensors (Stevens Hydraprobe) were positioned horizontally at 100 mm, 200 mm, and 500 mm into an undisturbed soil face at the edge-of-field.	Minimum value per day to capture the lowest value the volumetric water content drops to during the day
Soil temperature at 100, 200, and 500 mm (°C)	6/17/2020-12/31/2023	Sub-daily	Measurements were taken every thirty minutes.	Average daily value to capture the middle of the soil layer

**Table 2:** Management input data for study field 2016-2023. The period 2013-2015 was assumed to have identical management to 2019-2021.

Year	Crop	Inorganic Fertilizer (N rate kg/ha)	Inorganic Fertilizer (P rate (kg/ha)
2013	Soybean		
2014	Soybean	36	33
2015	Corn	211	
2016	Soybean		
2017	Corn/winter cover crops (cereal rye)	70	16
2018	Soybean	2	8
2019	Soybean		
2020	Soybean	36	33
2021	Corn	211	
2022	Soybean	9	19
2023	Corn	166	

## 2.1.3. SWAT model input data

**Table 3:** SWAT model inputs and settings.

General SWAT inputs	
Model version	SWAT2012 version 664 + Qi et al. (2016a,b; 2019) (SWAT-FT)
ArcGIS used	ArcMap - ArcSWAT 2012.10_8.26
SWAT watershed size ( $km^2$ )	0.0619 (single-field)
Timespan of model run	2013-2023 (3-year warm-up period)
Digital Elevation Model (DEM) ArcMap input	National Elevation Dataset (NED) 10 m. The DEM was modified to prevent the inclusion of roads in the model watershed.
Land use ArcMap input	National Agricultural Statistics Service Cropland Data Layer (NASS CDL) (NASS CDL, 2022)
Soils ArcMap input	Soil Survey Geographic (SSURGO) Database (SSURGO, 2024)
Air temperature data	2013-2023 NOAA-NCEI station data - USC00330563
Precipitation data	2013-2019 NOAA-NCEI station data - USC00330563 2020-2023 study site data. A standard rain gauge (NovaLynx 260-2510) and an Isco 674 tipping bucket rain gauge (Teledyne Isco) collected precipitation data at the edge-of-field next to the surface drainage outlet (Pease et al., 2018).
Tile drainage	900 mm depth and 30 ft drain spacing recommended by those monitoring the field site
Time step	Daily
Management	Management records were used as model inputs for 2016-2023. Years 2019-2021 were replicated for years 2013-2015 (Table 2).
Soil Stratification	To match soil test depths, the top layer of the SWAT soil profile (0-250 mm) was divided into 0-50.8 mm (0-2 in), 50.8-152.4 mm (2-6 in), and 152.4-250 mm. The other layers remained in their default intervals: 250-830 mm, 830-990 mm, and 990-2000 mm.

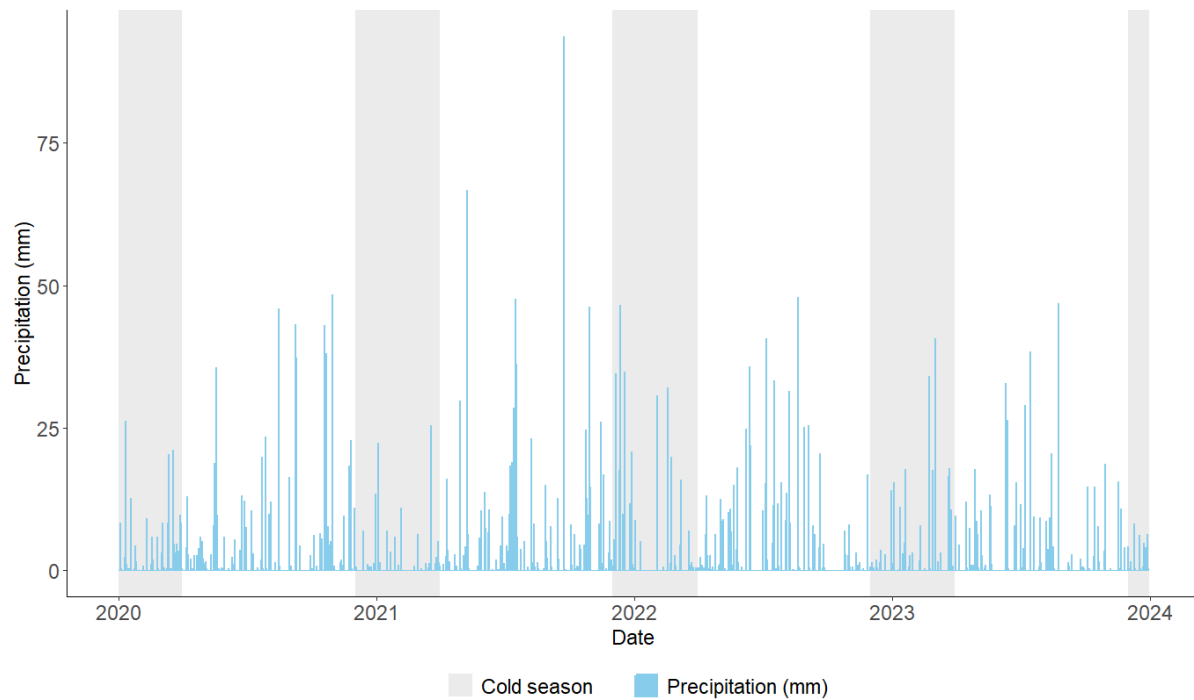


**Figure 2:** Precipitation over the period of time that there is measured data (2020-2023)

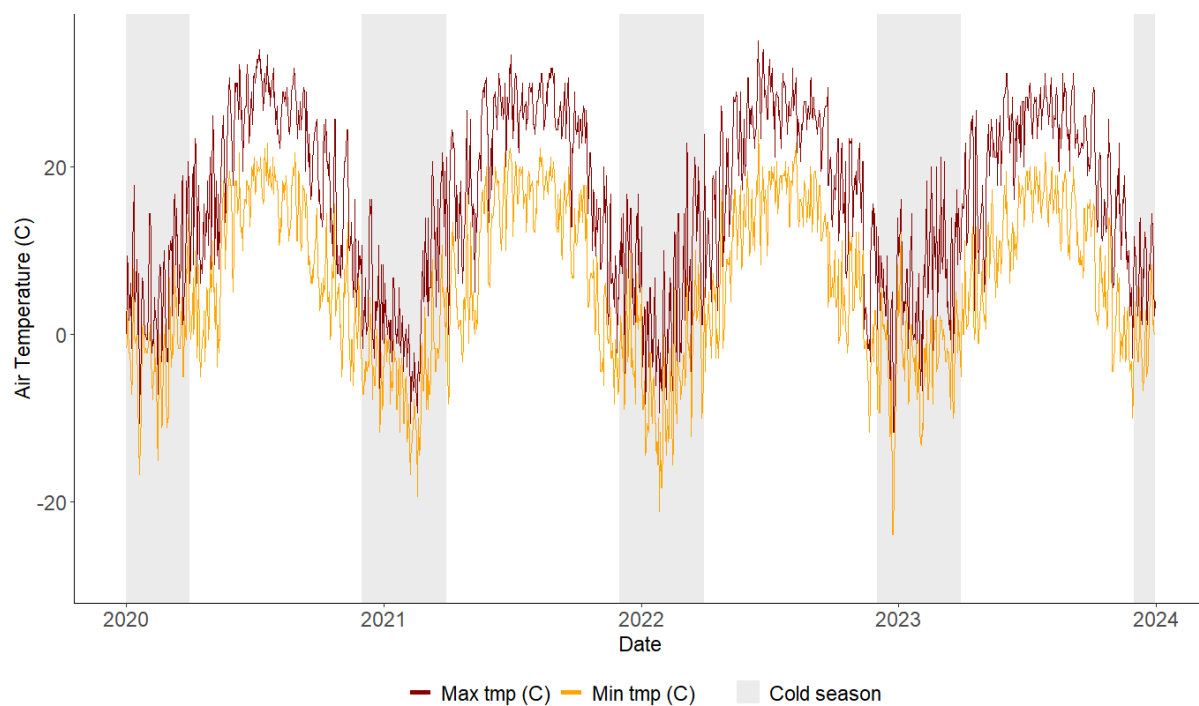


**Figure 3:** Minimum and maximum air temperature over the period of time that there is measured data (2020-2023)

Precipitation is particularly heavy in 2021 (Figure 2). Air temperature is slightly warmer in the 2022-2023 winter with the exception of a few very cold days (Figure 3).

**Table 4:** SWAT parameters, the initial and final values, the reason for the value change, and a description of the value. Complete .sol and .chm values can be found in the Appendix (6-7).

Parameter	SSURGO-Initialized Value	Final Value	Reasoning	Description
<b>Tile Drainage Depth (mm)</b>				
	NA	900	Value recommended by those monitoring field site (USDA-ARS)	The distance from the soil surface to the tile drains
<b>Tile drainage spacing (mm)</b>				
	NA	9144	Value recommended by those monitoring field site (USDA-ARS)	The distance between neighboring tile drains
<b>Drainage coefficient</b>				
	12.70	10	Value recommended by those monitoring field site (USDA-ARS)	A daily drainage coefficient
<b>Bulk density (g/cc)</b>				
10-50.8 mm	1.45	0.98	Soil measurement	Dry bulk density  More shallow soil layers typically have lower bulk density (NRCS, 2008).
50.8-152.40 mm	1.45	1.16	Soil measurement	
152.40-250.00 mm	1.45	1.25	Soil measurement	
250.00 - 830 mm	1.55	1.26	Calculated to produce reasonable field capacity values when compared to measured VWC	
830.00 - 990.00 mm	1.80	1.80	No measured data therefore left as SSURGO-initialized value	
990.00 - 2000 mm	1.90	1.90	No measured data therefore left as SSURGO-initialized	

			value	
<b>Ksat (mm/hr)</b>				
10.00 - 50.80 mm	33.01	20.32	Recommended by Monke et al., (1967) for the soil profile above the tile drains	Saturated hydraulic conductivity
50.80 - 152.40 mm	33.01	20.32	Recommended by Monke et al., (1967) for the soil profile above the tile drains	
152.40 - 250.00 mm	33.01	20.32	Recommended by Monke et al., (1967) for the soil profile above the tile drains	
250.00 - 830.00 mm	3.31	20.32	Recommended by Monke et al., (1967) for the soil profile above the tile drains	
830.00 - 990.00 mm	3.31	20.32	Recommended by Monke et al., (1967) for the soil profile above the tile drains	
990.00 - 2000 mm	2.66	2.66	Below the tile drains therefore left as SSURGO-initialized value	
<b>Average available water content</b>				
10-50.8 mm	0.21	0.21	Calculated to produce reasonable field capacity values when compared to measured VWC	Soil water available to plants
50.8-152.40 mm	0.21	0.21	Calculated to produce reasonable field capacity values when compared to measured VWC	
152.40-250.00 mm	0.21	0.26	Calculated to produce reasonable field capacity values when compared to measured VWC	
250.00 - 830 mm	0.15	0.28	Calculated to produce reasonable field capacity values when compared to measured VWC	
830.00 -	0.12	0.12	No measured VWC data	

990.00 mm			therefore left as the SSURGO-initialized value	
990.00 - 2000 mm	0.30	0.30	No measured VWC data therefore left as the SSURGO-initialized value	
<b>Clay/silt/sand (%)</b>				
10-50.8 mm	22.00/56.00/22.00	27.38/26.65/31.42	Soil measurement	Soil texture as a percentage of clay, silt, and sand particles
50.8-152.40 mm	22.00/56.00/22.00	26.65/51.90/21.45	Soil measurement	
152.40-250.00 mm	22.00/56.00/22.00	31.42/49.46/19.11	Soil measurement	
250.00 - 830 mm	42.00/42.00/16.00	34.32/48.32/17.35	Soil measurement	
830.00 - 990.00 mm	35.00/40.00/25.00	35.00/40.00/25.00	No measured data therefore left as the SSURGO-initialized value	
990.00 - 2000 mm	33.00/45.00/22.00	33.00/45.00/22.00	No measured data therefore left as the SSURGO-initialized value	
<b>Soil pH</b>				
10.00 - 50.80 mm	6.40	5.60	Soil measurement	How acidic or alkaline the soil is
50.80 - 152.40 mm	6.40	5.50	Soil measurement	
152.40 - 250.00 mm	6.40	6.30	Soil measurement	
250.00 - 830 mm	6.50	6.50	No measured data therefore left as the SSURGO-initialized value	
830.00 - 990.00 mm	7.60	7.60	No measured data therefore left as the SSURGO-initialized value	

990.00 - 2000 mm	8.00	8.00	No measured data therefore left as the SSURGO-initialized value	
<b>Organic carbon</b>				
10.00 - 50.80 mm	2.50	1.92	Converted from soil measurement organic matter (USDA NRCS, 2009)	Soil organic matter as a percentage of the soil
50.80 - 152.40 mm	2.50	1.34	Converted from soil measurement organic matter (USDA NRCS, 2009)	
152.40 - 250.00 mm	2.50	1.16	Converted from soil measurement organic matter (USDA NRCS, 2009)	
250.00 - 830.00 mm	0.50	0.50	No measured data therefore left as the SSURGO-initialized value	
830.00 - 990.00 mm	0.25	0.25	No measured data therefore left as the SSURGO-initialized value	
990.00 - 2000.00 mm	0.25	0.25	No measured data therefore left as the SSURGO-initialized value	
<b>Soil labile phosphorus (mg/kg)</b>				
10.00 - 50.80 mm	20.45	21.69	Converted from Mehlich-3 phosphorus measurement (Culman et al., 2019)	Initial phosphorus concentration in the soil (as a mass of phosphorus per mass of soil) that is available for plant uptake
50.80 - 152.40 mm	9.46	17.96	Converted from Mehlich-3 phosphorus measurement (Culman et al., 2019)	
152.40 - 250.00 mm	9.46	8.00	Converted from Mehlich-3 phosphorus measurement (Culman et al., 2019)	
250.00 - 830.00 mm	9.46	8.00	Assigned the same value as the 152.40 - 250.00 mm layer	

830.00 - 990.00 mm	9.46	8.00	Assigned the same value as the 152.40 - 250.00 mm layer	
990.00 - 2000.00 mm	9.46	8.00	Assigned the same value as the 152.40 - 250.00 mm layer	
<b>Soil NO3 (mg/kg)</b>				
10.00 - 50.80 mm	0.00	3.30	Soil measurement	Initial nitrogen concentration in the soil that is available for plant uptake
50.80 - 152.40 mm	0.00	3.30	Soil measurement	
152.40 - 250.00 mm	0.00	2.54	Soil measurement	
250.00 - 830.00 mm	0.00	2.54	Assigned the same value as the 152.40 - 250.00 mm layer	
830.00 - 990.00 mm	0.00	2.54	Assigned the same value as the 152.40 - 250.00 mm layer	
990.00 - 2000.00 mm	0.00	2.54	Assigned the same value as the 152.40 - 250.00 mm layer	

The full soil and chemistry (.sol and .chm) SWAT input files can be found in the appendix (Appendix 6-7).

## 2.2. Improvements to soil temperature simulation in the SWAT source code

To improve the simulation of cold season processes in SWAT, Qi et al. (2016a,b; 2019) developed a new approach to simulate heat transfer within the soil profile in SWAT2012. The approach uses a physically-based one-dimensional soil-temperature equation that takes into account the heat transfer within the soil profile, soil moisture, and soil water phase changes (Figure 4). The new physically based equation estimates snow and soil surface temperatures more accurately by taking into account heat exchange and latent heat. The algorithm also integrates soil water freeze-thaw, soil ice content, moisture,

and snow density when calculating soil heat conduction between layers into the model. These resulted in a better representation of soil temperature, percolation through the soil, lateral flow, runoff from the surface, and discharge from groundwater (Qi et al., 2019).

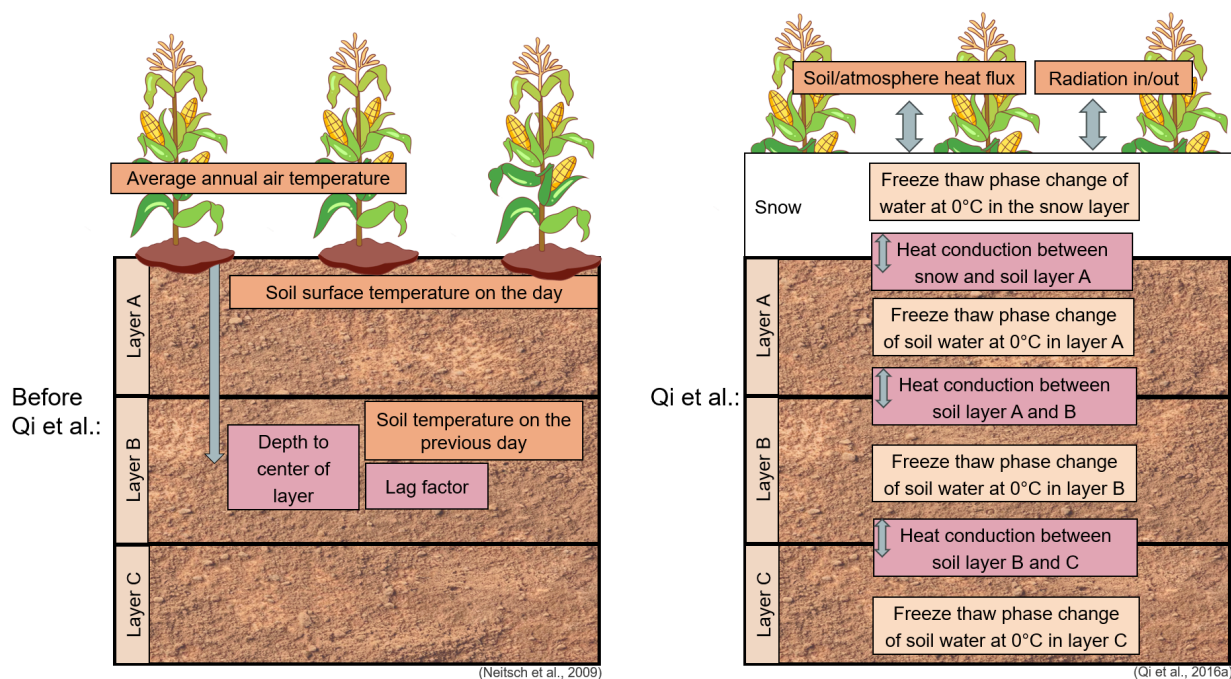


**Figure 4:** A representation of the soil temperature algorithm before and after the addition of Qi's physically-based equation for one-dimensional heat transfer (Neitsch et al., 2009; Qi et al., 2016a).

The SWAT2012 limitations to soil temperature simulation also apply to the SWAT+ source code (SWAT+ source code version 61.0.2).

### 2.3. Improvements to the perched water table algorithm in the SWAT source code

The following perched water table algorithms can be found in the permain.f source code. The basin.bsn SWAT input file has a parameter called IWTDN. IWTDN determines which perched water table algorithm is used in the permain.f file. A history of other perched water table algorithms used in SWAT by research teams can be found in the Appendix (1-4).

### 2.3.1. Revised Modified DRAINMOD Approach

The perched water table depth algorithm used in SWAT2009 and SWAT2012 (IWTDN=1), titled the Revised Modified DRAINMOD Approach (Moriassi et al., 2011), is based on soil water change in the entire profile multiplied by a water table depth adjustment factor. The Revised Modified DRAINMOD Approach is a more recent iteration of the Modified DRAINMOD Approach (Appendix 4). Unlike the Modified DRAINMOD Approach, in the Revised Modified DRAINMOD Approach the water table depth adjustment factor is automatically calculated based on effective porosity within a soil layer. The Kalcic Lab made modifications to the Revised Modified DRAINMOD Approach to prevent the perched water table from going above the soil surface or below the impervious layer.

In the Revised Modified DRAINMOD Approach (Moriassi et al., 2011), the perched water table is initialized one time at the beginning of the simulation. Then, the “delta” change in soil water every day is calculated by subtracting the soil water stored in the entire profile on the current day from the soil water stored in the entire profile on the previous day.

$$\Delta spw = spw_{t-1} - spw_t$$

Where  $\Delta spw$  is the change in soil water from the previous day to the current day in the whole soil profile (mm),  $spw_{t-1}$  is the soil water at the previous time step in the whole SWAT soil profile (mm), and  $spw_t$  is soil water at the current time step in the whole SWAT soil profile (mm).

A water table factor is automatically calculated for each soil layer based on the effective porosity of that layer. The water table factor used is the equation for the layer the water table was in on the previous day. This equation was updated from the Moriassi et al. (2011) paper to match the equation in the SWAT source code version 644.

$$wtfctr = 437.13(efpor)^2 - 95.08(efpor) + 8.257$$

Where  $wfctr$  is a water table factor that adjusts soil water, and  $efpor$  is the effective porosity of the soil layer the water table was in on the previous day ( $\frac{mm\ H2O}{mm\ soil}$ ).

$wfctr$  is used to calculate perched water table depth by:

1. Calculating the change in water table depth on the current day by multiplying the change in soil water by the water table factor:

$$\Delta wtdpth = wfctr \times \Delta spw$$

Where  $\Delta wtdpth$  is the change in water table depth from the previous day to the current day (mm),  $wfctr$  is a water table factor that adjusts soil water, and  $\Delta spw$  is the change in soil water from the previous day to the current day in the whole soil profile (mm).

2. Calculating the perched water table depth by adding the change in water table depth to the depth of the water table on the previous day. If it is below the impervious layer, water table depth is set to 0.

$$wtdpth_t = wtdpth_{t-1} + \Delta wtdpth, \quad \text{if } wtdpth_t \geq imp$$

$$wtdpth_t = 0, \quad \text{if } wtdpth_t < imp$$

Where  $wtdpth_t$  is the depth of the perched water table at the current time step (mm),  $wtdpth_{t-1}$  is the depth of the perched water table at the previous time step (mm),  $\Delta wtdpth$  is the change in water table depth from the previous day to the current day (mm), and  $imp$  is the depth to the impervious layer from the soil surface (mm).

Example of IWTDN=1:

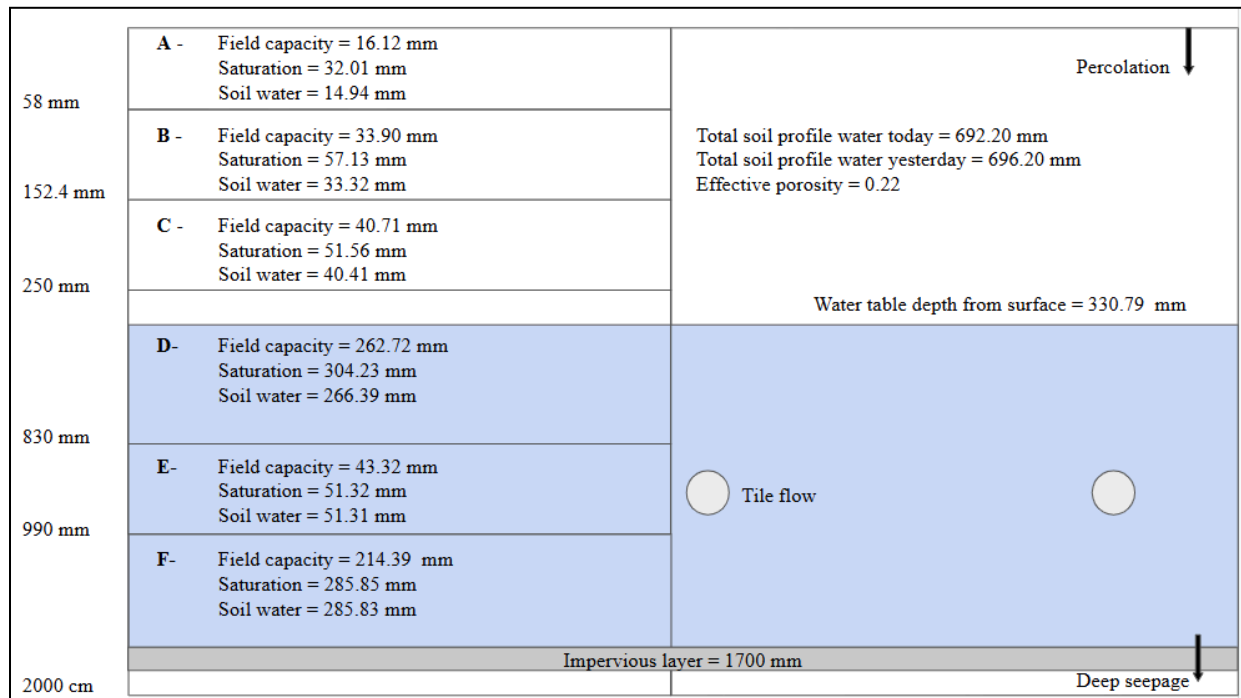


**Figure 5:** Example of the perched water table calculations in the Revised modified DRAINMOD approach.

- Calculate change in soil water (distance from soil surface) from the previous day
  - $692.20 \text{ mm} - 696.20 \text{ mm} = 4 \text{ mm}$
- Calculate the water table factor
  - $wtfctr = 437.13(0.22)^2 - 95.08(0.22) + 8.257 = 8.55$
- Calculate the change in water table depth
  - $4 \text{ mm} \times 8.55 = 34.18 \text{ mm}$
- Add or subtract the change in water table depth from yesterday's water table depth
  - $296.61 \text{ mm} + 34.18 \text{ mm} = 330.79 \text{ mm from the soil surface}$

### 2.3.2. Kalcic Lab improvements to perched water table depth calculation

The Kalcic Lab modified how perched water table depth is calculated to make it more physically based and dependent on soil moisture above the impermeable layer on a given day (IWTDN=2). The updated water table depth calculations are as follows:

First, drainable porosity is calculated for each layer starting at the bottom of the soil profile. Drainable porosity is equal to the difference between saturation and field capacity for a layer, and it is the available space for storing drainable water. If the impervious layer is within the current layer, then multiply drainable porosity by the fraction of the layer more shallow than the impervious layer.

$$dpor_l = slst - slfc, \quad \text{if imp is deeper than layer}$$

$$dpor_l = (slst - slfc) \times \left( \frac{imp - hght_t}{hght_b - hght_t} \right), \quad \text{if imp is within layer}$$

Where  $dpor_l$  is drainable porosity in a layer (mm),  $slst$  is saturation in the current soil layer (mm),  $slfc$  is field capacity in the current soil layer (mm),  $hght_b$  is the distance from the soil surface to the bottom of the current soil layer (mm),  $hght_t$  is the distance from the soil surface to the top of the current soil layer (mm), and  $imp$  is the distance from the soil surface to the impervious layer (mm).

Second, each day the sum of excess soil moisture (soil moisture above field capacity) is calculated starting at the impermeable layer or the bottom of the soil profile, whichever is shallower, up to the soil surface. If the impervious layer is within a soil layer, the excess is calculated in that layer and then multiplied by the fraction of the soil layer above the impervious layer.

*if sol sw > sol fc in a soil layer*

$$exsm_l = (slw - slfc), \quad \text{if layer is above imp}$$

$$exsm_l = (slw - slfc) \times \left( \frac{imp - hght_t}{hght_b - hght_t} \right), \quad \text{if imp is within layer}$$

$$exsm = \sum_{\substack{\text{soil surface} \\ \text{soil layer} = i}} exsm_l$$

Where  $exsm_l$  is the excess soil moisture in the soil profile above field capacity in a certain layer (mm),  $exsm$  is the total excess soil moisture in the soil profile above the impervious layer (mm),  $slw$  is the soil moisture in the current soil layer (mm),  $slst$  is saturation in the current soil layer (mm),  $slfc$  is field capacity in the current soil layer (mm),  $hght_b$  is the distance from the soil surface to the bottom of the current soil layer (mm),  $hght_t$  is the distance from the soil surface to the top of the current soil layer (mm), and  $imp$  is the distance from the soil surface to the impervious layer (mm).

Third, water table depth is initialized at the impervious layer or at the bottom of the soil profile, whichever is shallower. The water table cannot be initialized below the SWAT soil profile in this algorithm because the moisture content of the soil profile below the bottom of the SWAT soil profile is not simulated. The calculation of perched water table depth is only concerned with the soil profile above the impervious layer.

$$wt = solprofile_b, \quad \text{if } imp > solprofile_b$$

$$wt = imp, \quad \text{if } imp < solprofile_b$$

$$hght_b = imp, \quad \text{if } imp \text{ is within the current soil layer}$$

Where  $wt$  is the distance from the soil surface to the top of the perched water table (mm),  $hght_b$  is the distance from the soil surface to the bottom of the current soil layer (mm),  $imp$  is the distance from the soil surface to the impervious layer (mm), and  $solprofile_b$  is the distance from the soil surface to the bottom of the soil profile (mm).

Now that the excess soil moisture above the impermeable layer and the drainable pore space above the impermeable layer is known, perched water table depth can be calculated by hypothetically reallocating excess moisture to the deepest possible station within a soil layer above the impermeable layer.

Starting at the layer containing the impermeable layer or the deepest soil layer, whichever is shallower, if the excess total soil moisture that was calculated above the impermeable layer exceeds the drainable porosity for that layer, use part of the total excess water to fill the drainable porosity for that layer and raise the water table to the top of that layer. This process is repeated, moving shallower in the soil profile, until there is not enough excess soil moisture to fill the drainable porosity in a layer. When a layer is reached where remaining excess soil moisture is less than the available drainable porosity, the fraction of filled drainable pore space is multiplied by the height of the layer.

$$\text{if } exsm_{t-1} > dpor_l$$

$$wt = hght_t$$

$$exsm_t = exsm_{t-1} - dpor_l$$

$$\text{if } exsm_{t-1} < dpor_l$$

$$frctn = \frac{exsm_{t-1}}{dpor_l}$$

$$wt\ tbl_t = wt\ tbl_{t-1} - (hght_t - hght_b) \times frctn$$

$$exsm_t = 0$$

Where  $wt$  is the distance from the soil surface to the top of the perched water table (mm),  $frctn$  is the fraction of filled pore space between field capacity and saturation,  $exsm_t$  is the excess soil moisture in the current time step (mm),  $exsm_{t-1}$  is the excess soil moisture in the previous time step (mm),  $dpor_l$  is drainable porosity in that layer (mm),  $hght_t$  is the distance from the soil surface to the top of the current

soil layer (mm), and  $hght_b$  is the distance from the soil surface to the bottom of the current soil layer (mm).

Example of IWTDN=2:

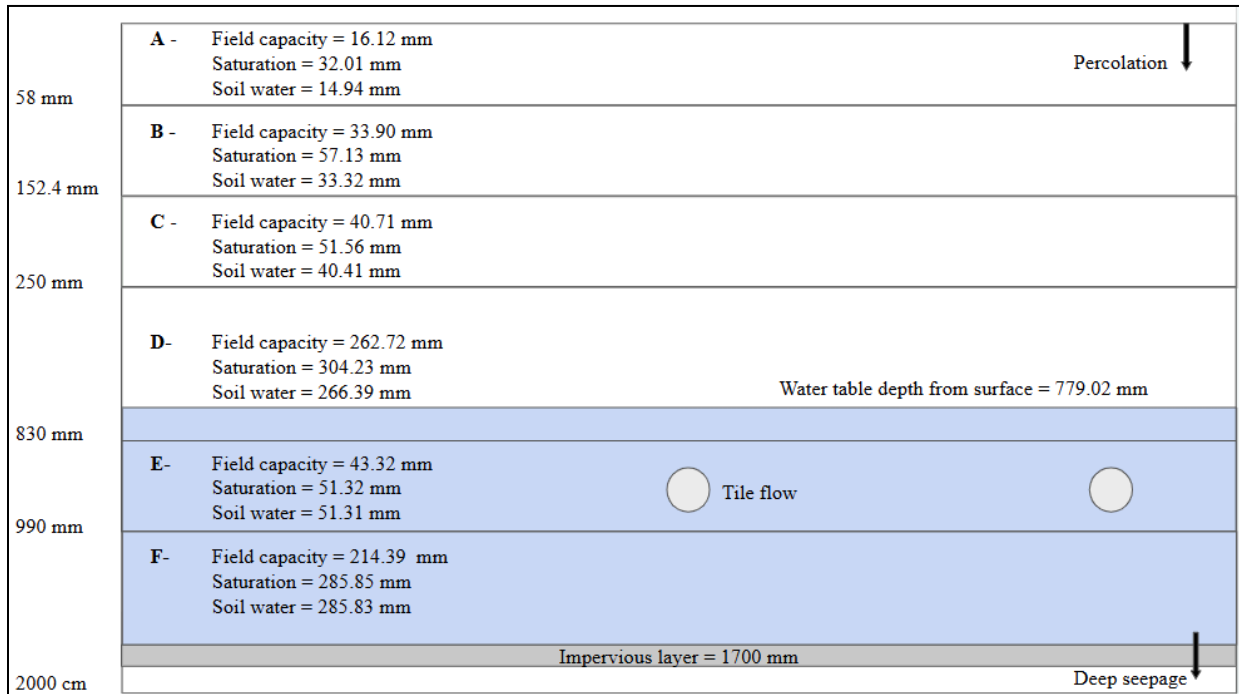


**Figure 6:** Example of the perched water table calculations in the Kalcic Lab approach.

1. Drainable porosity for each layer is calculated (note this does not change over time)

$$a. A = 32.01 \text{ mm} - 16.12 \text{ mm} = 15.89 \text{ mm}$$

$$b. B = 57.13 \text{ mm} - 33.90 \text{ mm} = 23.23 \text{ mm}$$

$$c. C = 51.56 \text{ mm} - 40.71 \text{ mm} = 10.85 \text{ mm}$$

$$d. D = 304.23 \text{ mm} - 262.72 \text{ mm} = 41.50 \text{ mm}$$

$$e. E = 51.32 \text{ mm} - 43.32 \text{ mm} = 8.00 \text{ mm}$$

$$f. F = (285.85 \text{ mm} - 214.39 \text{ mm}) \times \left( \frac{1700 \text{ mm} - 990 \text{ mm}}{2000 \text{ mm} - 990 \text{ mm}} \right) = 50.28 \text{ mm}$$

2. Excess soil water (drainable water) above field capacity is summed

$$a. ((285.83 - 214.39) \times \frac{1700 - 990}{2000 - 990}) + (51.31 - 43.32) +$$

$$(266.39 - 262.72) = 61.93 \text{ mm}$$

3. Starting at the impervious layer, if total excess soil water is greater than drainage porosity in that soil layer, the water table is set to the top of the layer.
  - a. In soil layer F,  $61.93 \text{ mm} > 50.28 \text{ mm}$ . The water table is set to 990 mm and there is 11.65 mm of excess soil water remaining.
  - b. In soil layer E,  $11.65 \text{ mm} > 8 \text{ mm}$ . The water table is set to 830 mm and there is 3.65 mm of excess soil water remaining.
  - c. In soil layer D,  $3.65 \text{ mm} < 41.50 \text{ mm}$  so the water table depth will be calculated in this layer.
    - i.  $\frac{3.65}{41.5} = 0.09$
    - ii.  $830 \text{ mm} - 250 \text{ mm} = 580 \text{ mm}$
    - iii.  $580 \text{ mm} \times 0.09 = 50.98 \text{ mm}$
    - iv.  $830 \text{ mm} - 50.98 \text{ mm} = 779.02 \text{ mm from the soil surface}$

The SWAT2012 limitations to perched water table depth simulation also apply to the SWAT+ source code (SWAT+ source code version 61.0.2).

### 2.3.3. Tile flow calculation

After the water table depth from the soil surface is calculated for the day, tile drainage is calculated in the drains.f file using an updated tile drain method from Moriasi et al. (2007a; 2012). The drains.f file uses Kirkham (1957) and Hooghoudt (1940) equations from DRAINMOD (Skaggs, 1978) and applies them to the SWAT program. The Kirkham equations are relevant when there is surface ponding and more complex hydrologic situations. The Hooghoudt equations are used when there is minimal ponding and the water table is deeper than the soil surface. The rate of water reaching the tiles is dependent on lateral hydraulic conductivity in the saturated zone, water table height from the impervious layer, distance between tile

drains, tile drain depth from soil surface, and soil profile layer and profile depth. How much water flows through the tile drains is then calculated using the hydraulic head within the tile drains, the water table height, and either the Hooghoudt or Kirkham equations (Moriasi et al., 2007a; Moriasi et al., 2012). The Kalcic Lab also fixed a tile drain bug in all versions of SWAT code used in this thesis to only allow tile drains to use water from soil above the tile drains.

#### 2.4. Model calibration and validation

Four SWAT executables were calibrated and validated in order to compare results between the executables (Figure 7).

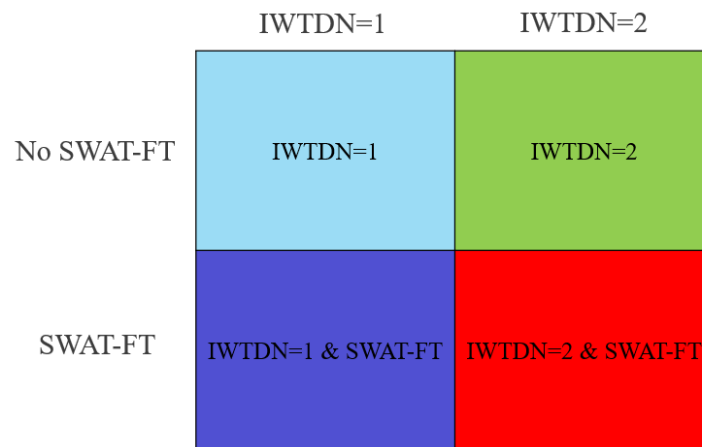


**Figure 7:** The four SWAT executables tested in this thesis

1. No Improvements (*IWTDN=1*)
  - a. The *IWTDN=1* executable has no changes to the soil temperature or perched water table algorithms from the SWAT version 664, except a bug fix to limit the perched water table to exist between the soil surface and the impermeable layer.
2. Only Qi et al. (2016a,b; 2019) improvements to the calculation of soil temperature (*IWTDN=1* & *SWAT-FT*)
  - a. The *IWTDN=1* & *SWAT-FT* executable has the improvements to the simulation of soil temperature and heat transfer from Qi et al (2016a,b; 2019) integrated into the SWAT

source code as well as a bug fix to limit the perched water table to exist between the soil surface and the impermeable layer.

3. Only improvements to the simulation of the shallow water table (*IWTDN=2*)
  - a. The *IWTDN=2* executable has the improvements to the perched water table calculations.
4. All improvements (*IWTDN=2* & *SWAT-FT*)
  - a. The *IWTDN=2* & *SWAT-FT* executable has both the temperature and perched water table improvements to the source code.

Eight model outputs were selected based on available field data (Table 1):

- Tile flow (mm)
- Perched water table depth (mm)
- Volumetric water content (mm/mm) at 100 mm
  - The SWAT model source code was modified to divide layer soil water content values (mm) by the depth from the top to the bottom of the layer (mm) to produce volumetric water content (mm/mm).
- Volumetric water content (mm/mm) at 200 mm
  - The SWAT model source code was modified to divide layer soil water content values (mm) by the depth from the top to the bottom of the layer (mm) to produce volumetric water content (mm/mm).
- Volumetric water content (mm/mm) at 500 mm
  - The SWAT model source code was modified to divide layer soil water content values (mm) by the depth from the top to the bottom of the layer (mm) to produce volumetric water content (mm/mm).
- Soil temperature (°C) at 100 mm
- Soil temperature (°C) at 200 mm
- Soil temperature (°C) at 500 mm

Parameters for calibration were selected from a subset of the parameters used in Apostel et al. (2021) along with other parameters that applied to a single-field-model and were relevant to the outputs of interest (Table 5).

**Table 5:** Description of parameters for calibration, original values, calibration ranges, reasoning for selecting the range, and a description of the parameter being used.

Parameter	Orig. Value	Bounds	Range Justification	Parameter Description
SFTMP.bsn	3	-3,3	Included default and final parameters from Apostel et al. (2021)	The air temperature where precipitation can be snow or rain (°C)
SMTMP.bsn	3	-3,3	Included default and final parameters from Apostel et al. (2021)	The temperature snow melts (°C)
TIMP.bsn	0.4	0.01,0.4	Included default and final parameters from Apostel et al. (2021)	A lag factor for snow temperature
SMFMX.bsn	6.9	1.4,6.9	Default range	A melt factor on June 21 (mm water/°C-day)
SMFMN.bsn	6.9	1.4,6.9	Default range	A melt factor on December 21 (mm water/°C-day)
SNOCOVMX.bsn	6	0.8,6	Included default and final parameters from Apostel et al. (2021)	Depth of snow which provides 100% cover
SNO50COV.bsn	0.7	0.2,0.7	Included default and final parameters from Apostel et al. (2021)	Fraction of SNOCOVMX that covers 50% of the

				ground
ESCO.hru	1	0.001,1	Default range	The soil profile evaporation parameter
EPCO.hru	1	0,1	Default range	The water uptake parameter for plants
R2ADJ.hru	1	0,1	Default range	A curve number retention parameter which adjusts for flat and poorly draining soils  This was uncommented in the source code to allow it to be used.
OV_N.hru	0.5	0.05,0.5	Based on an approximate range for agricultural land (SWAT 2009 Documentation; Engman, 1986)	Manning's "n" value for overland flow
DEP_IMP.hru	2133.6	1524,2133.6	Site measurement was taken at 1524 mm depth and measured data showed the water table dipped below 1524 mm	The depth from the soil surface to the impervious layer
CN2.mgt	89	84,94	+/- 5 from the default SWAT value	The initial curve number for moisture condition II
LATKSATF.sdr	4	1,4	Default SWAT range with bottom 0.01-1 removed due to being unreasonable for a soil that would be expected to have lateral conductivity at least as high as vertical	Lateral saturated hydraulic conductivity
SOL_CRK.sol	0.5	0,0.5	Default range	Soil profile crack volume potential

#### 2.4.1. Using SWATrunR for model calibration

SWAT model calibration and validation was executed using SWATrunR, an R package that allows the user to perform numerous SWAT runs using a custom range of parameters (Schürz, 2019). The extensive modification of the SWAT source code and the new model outputs required a flexible calibration approach, and SWATrunR allowed for the customization of output files and new parameters. R version 4.2.2 and SWATrunR version SWATplusR 0.6.4 was used (Schürz, 2019; R Core Team, 2024). A bug in the 0.6.4 SWATrunR source code prevented SWATrunR from reading values in the output.sol file. The SWATrunR source code was modified to be able to read the ANION\_EXCL and SOL\_CRK parameters (Appendix 5).

The calibration and validation period for model outputs varied based on measured data availability (Table 6). All calibration periods began as close to the beginning of the water year in 2021 as available data allowed. Perched water table depth from the soil surface was not validated due to limited data availability.

**Table 6:** Calibration and validation periods for each model output.

Output	Calibration period	Validation period
Tmp (°C) at all depths	10/01/2021-12/31/2023	6/17/2020-09/30/2021
Tile flow (mm)	10/01/2021-12/31/2023	01/01/2020-09/30/2021
Water table (mm)	5/12/2022-12/31/2023	
VWC at all depths	10/01/2021-12/31/2023	6/17/2020-09/30/2021

Thirty thousand parameter combinations were selected from within the bounds (Table 5) using latin hypercube sampling. Then, the root mean squared error standardized by standard deviation (RSR) was calculated for each of the thirty thousand runs and each of the eight model output during the calibration periods. RSR was chosen because it is a commonly used statistic for model performance evaluation (Chu and Shirmohammadi, 2004; Singh et al., 2004; Vasquez-Amábile and Engel, 2005; Moriasi et al., 2007b).

The closer the RSR value is to 0, the better the model performance. The calibration runs were ranked from best RSR score to worst for each output. Then, the ranks were summed for each run to generate a total score per run where the runs with the best statistical outcomes had smaller sums. The calibrated run for the executable was selected by sorting for the smallest sum. The calibration process was repeated for each of the four executables as well as for the validation period. Additional model statistics not used for model calibration are reported in the Appendix (8-11).

#### 2.4.2. Model evaluation

The four model executables were compared using three combinations. First, the *IWTDN=1 & SWAT-FT* executable was compared to the *IWTDN=1* executable to highlight the difference in outputs created by integrating the Qi et al. (2016a,b; 2019) SWAT-FT improvements. Then, the *IWTDN=2 & SWAT-FT* executable was compared to the *IWTDN=1 & SWAT-FT* executable to highlight the difference in outputs created by the new shallow water table algorithm improvements (*IWTDN=2*). Lastly, the *IWTDN=1* executable was compared to the *IWTDN=2* executable to evaluate the new shallow water table algorithm in the absence of the SWAT-FT improvements.

### 3. Results

Final calibration results for the 15 SWAT parameters were determined for all four executables (*IWTDN=1, IWTDN=1 & SWAT-FT, IWTDN=2, IWTDN=2 & SWAT-FT*) and led to a mix of “satisfactory” and “unsatisfactory” RSR statistics for both calibration and validation of the eight outputs (Tables 8:10). Time series graphs were also constructed to compare executable trends across calibration and validation periods from 2020 through the end of 2023 (Figures 8:20).

**Table 7:** Model calibration results for 15 SWAT parameters.

Parameter	Bounds	Orig Value	IWTDN=1	IWTDN=1 & SWAT-FT	IWTDN=2	IWTDN=2 & SWAT-FT
SFTMP.bsn	-3,3	3	1.8834	2.7512	-1.6774	2.6582
SMTMP.bsn	-3,3	3	-2.9471	1.9517	-1.9930	2.3850
TIMP.bsn	0.01,0.4	0.4	0.2522	0.1728	0.0954	0.1666
SMFMX.bsn	1.4,6.9	6.9	5.8873	3.8176	4.4951	5.6664
SMFMN.bsn	1.4,6.9	6.9	6.8292	4.1313	5.6003	2.6958
SNOCVMX.bsn	0.8,6	6	3.7536	4.3290	2.7965	3.4942
SNO50COV.bsn	0.2,0.7	0.7	0.5670	0.3053	0.6013	0.3568
ESCO.hru	0.001,1	1	0.8177	0.4154	0.9056	0.5735
EPCO.hru	0,1	1	0.7448	0.4965	0.5629	0.0942
R2ADJ.hru	0,1	1	0.7529	0.7857	0.2392	0.3026

OV_N.hru	0.05,0.5	0.5	0.0514	0.1181	0.4541	0.4742
DEP_IMP.hru	1524,2133 .6	2133.6	1709.832	1556.925	1544.322	1700.667
CN2.mgt	84,94	94	93.4955	88.2624	89.8425	89.2654
LATKSATF.sdr	1,4	4	2.4566	3.7260	1.4904	1.1721
SOL_CRK.sol	0,0.5	0.5	0.0207	0.0087	0.2058	0.2627

### 3.1. Evaluating soil temperature improvements made by Qi et al. (2016a,b; 2019)

Integration of the Qi et al. (2016a,b; 2019) algorithm (*IWTDN=1 & SWAT-FT*) improved the RSR score for soil temperature at all depths, perched water table simulation, and volumetric water content at 200 mm (Table 8). Tile flow, volumetric water content at 100 mm, and volumetric water content at 500 mm produced similar RSR values for *IWTDN=1* and *IWTDN=1 & SWAT-FT* (Table 8). A satisfactory RSR score at the watershed scale in a monthly time interval is 0.7 (Moriasi et al., 2007b). Validation of the Qi et al. (2016a,b; 2019) algorithm (*IWTDN=1 & SWAT-FT*) improved the RSR score across all outputs over *IWTDN=1*, except for tile flow outputs, which stayed statistically similar. Only the temperature outputs at three depths and calibration values for volumetric water content at 500 mm had “satisfactory” RSR results.

**Table 8:** RSR scores comparing eight SWAT outputs across two executables. The two executables compared are (1) the *IWTDN=1 & SWAT-FT* executable (represented by the dark blue line in figures 8-11) and (2) the *IWTDN=1* executable (represented by the light blue line in figures 8-11). Moriasi et al. (2007b) indicates that 0.7 and less is a satisfactory RSR at the watershed scale in a monthly time interval. Moriasi (2007) considers a RSR of 0.5 and less to be very good. Satisfactory values are in bold.

Output	Calibration		Validation		Satisfactory RSR
	IWTDN=1	IWTDN=1 & SWAT-FT	IWTDN=1	IWTDN=1 & SWAT-FT	
Tmp (°C) at 100 mm	<b>0.3553</b>	<b>0.2142</b>	<b>0.3471</b>	<b>0.2760</b>	< 0.7
Tmp (°C) at 200 mm	<b>0.3010</b>	<b>0.2032</b>	<b>0.3042</b>	<b>0.2544</b>	< 0.7
Tmp (°C) at 500 mm	<b>0.3312</b>	<b>0.2784</b>	<b>0.3483</b>	<b>0.2838</b>	< 0.7
Tile flow (mm)	0.9925	1.0653	1.0861	1.0807	< 0.7
Water table (mm)	1.0611	0.9035			< 0.7
VWC at 100 mm ( <i>mm/mm</i> )	0.9732	0.9473	0.9311	0.7170	< 0.7
VWC at 200 mm ( <i>mm/mm</i> )	2.6028	1.6245	3.2884	2.8637	< 0.7
VWC at 500 mm ( <i>mm/mm</i> )	<b>0.6260</b>	<b>0.6789</b>	2.1676	1.8483	< 0.7

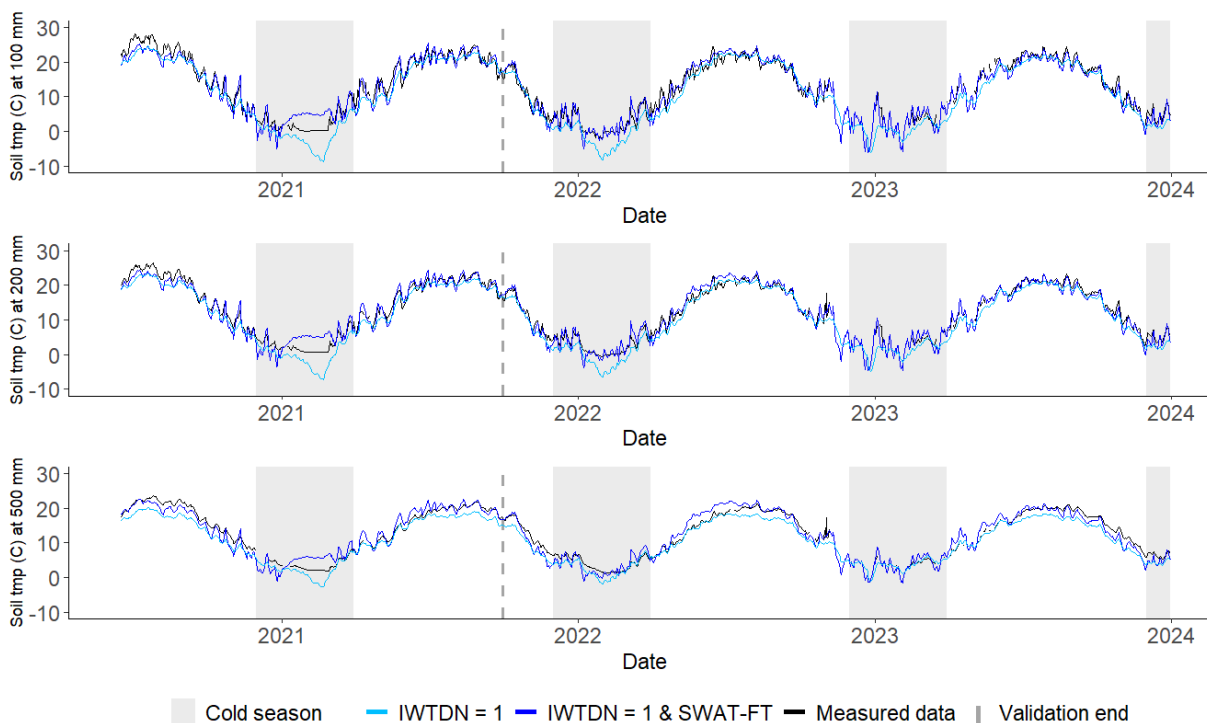


**Figure 8:** Time series of soil temperature ( $^{\circ}\text{C}$ ) at 100 mm, 200 mm, and 500 mm from June 2020 through the end of 2023. Measured data is represented by the black line, the *IWTDN=1* & *SWAT-FT* output is represented by the dark blue line, and the *IWTDN=1* output is represented by the light blue line. The validation period (ends 09/30/2021) is separated from the calibration period (starts 10/01/2021) by the vertical dashed line. Cold seasons (12/1-3/31) are highlighted in grey.

The *SWAT-FT* improvements (*IWTDN=1* & *SWAT-FT*) show improvement in soil temperature simulation compared to the executable without the *SWAT-FT* improvements (*IWTDN=1*) for both calibration and validation periods (Table 8). All layers and executables that simulate soil temperature are within the “satisfactory” RSR score bounds for both calibration and validation periods (Table 8). In the time series graph, the executable with *SWAT-FT* visually shows improvement in the cold seasons when the dark blue line is closer to measured data during the cold season of 2022 and 2023 (Figure 8). Statistically, during the calibration period in the cold season, RSR is improved at the 100 mm and 200 mm layers, while the 500 mm layer produced similar statistics (Table 11). In the 500 mm layer, there is also visually an improvement in soil temperature simulation during the summer months across the calibration and validation period (Figure 8).

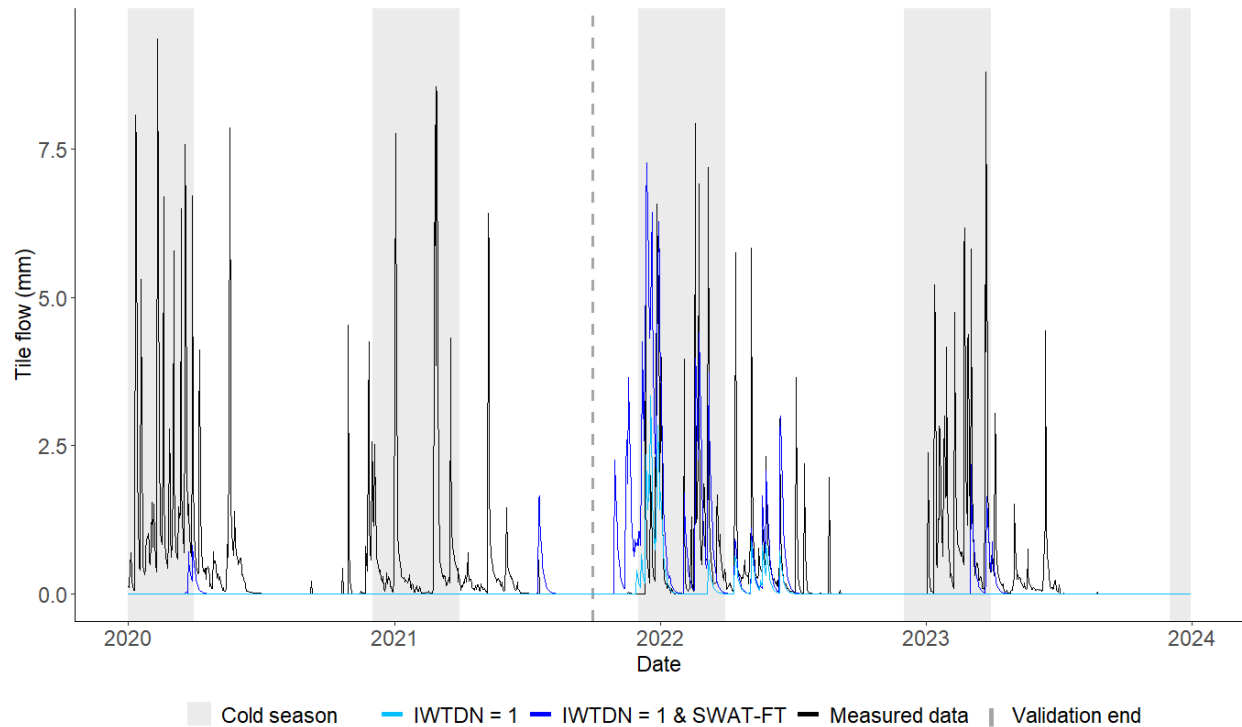


**Figure 9:** Time series of flow through the tile drains (mm) from January 2020 through the end of 2023. Measured data is represented by the black line, the *IWTDN=1 & SWAT-FT* output is represented by the dark blue line, and the *IWTDN=1* output is represented by the light blue line. The validation period (ends 09/30/2021) is separated from the calibration period (starts 10/01/2021) by the vertical dashed line. Cold seasons (12/1-3/31) are highlighted in grey.

RSR scores do not fall within the “satisfactory” RSR score bounds for tile flow for *IWTDN=1 & SWAT-FT* or *IWTDN=1*. RSR scores are also similar across the calibration and validation periods for both executables (Table 8). In the time series graph, the improvements to tile flow from integrating the *SWAT-FT* improvements are evident when the *IWTDN=1 & SWAT-FT* executable simulates peaks in tile flow that are consistent with the measured data, while the *IWTDN=1* executable does not simulate any tile flow (mid 2020, late 2021, early 2023). This is consistent across the calibration and validation period (Figure 9).

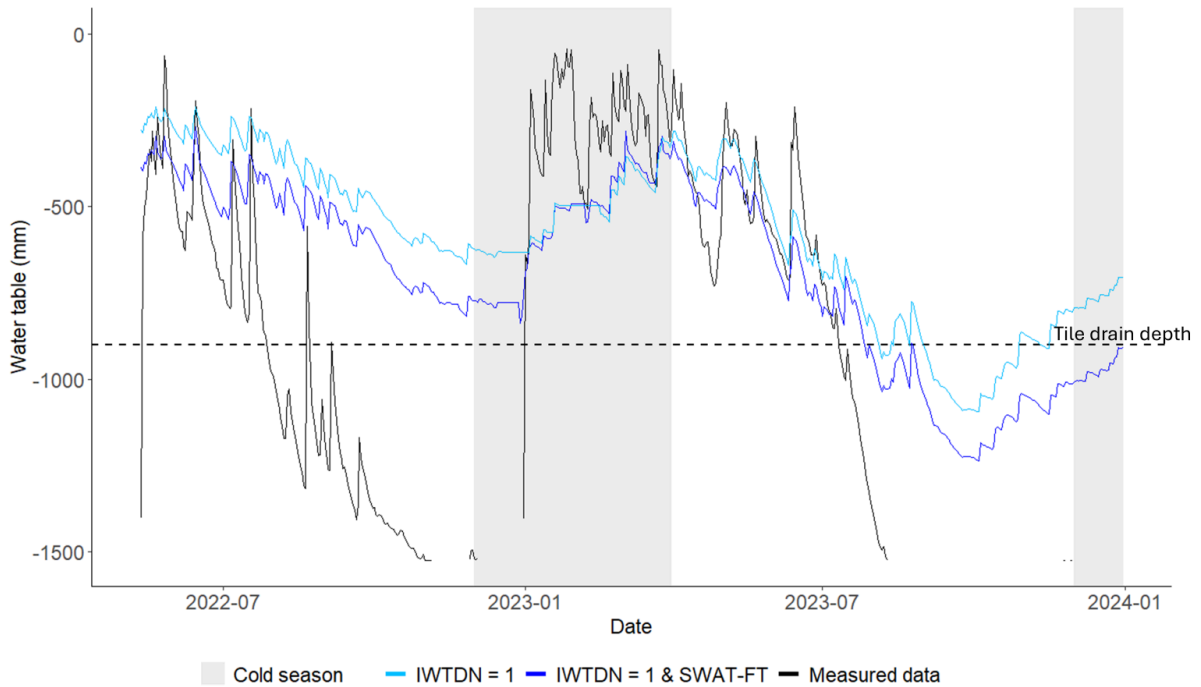


**Figure 10:** Time series of perched water table depth from the soil surface (mm) from May 2022 through the end of 2023. Measured data is represented by the black line, the *IWTDN=1 & SWAT-FT* output is represented by the dark blue line, and the *IWTDN=1* output is represented by the light blue line. Cold seasons (12/1-3/31) are highlighted in grey.

Shallow water table depth (mm) shows some statistical improvement in RSR when the SWAT-FT improvements are included in the executable (Table 8). The RSR values do not fall within the “satisfactory” range (Table 8). However, it was noticed that there was variability in model performance for water table comparison between *IWTDN=1 & SWAT-FT* and *IWTDN=1* depending on parameter set selection.

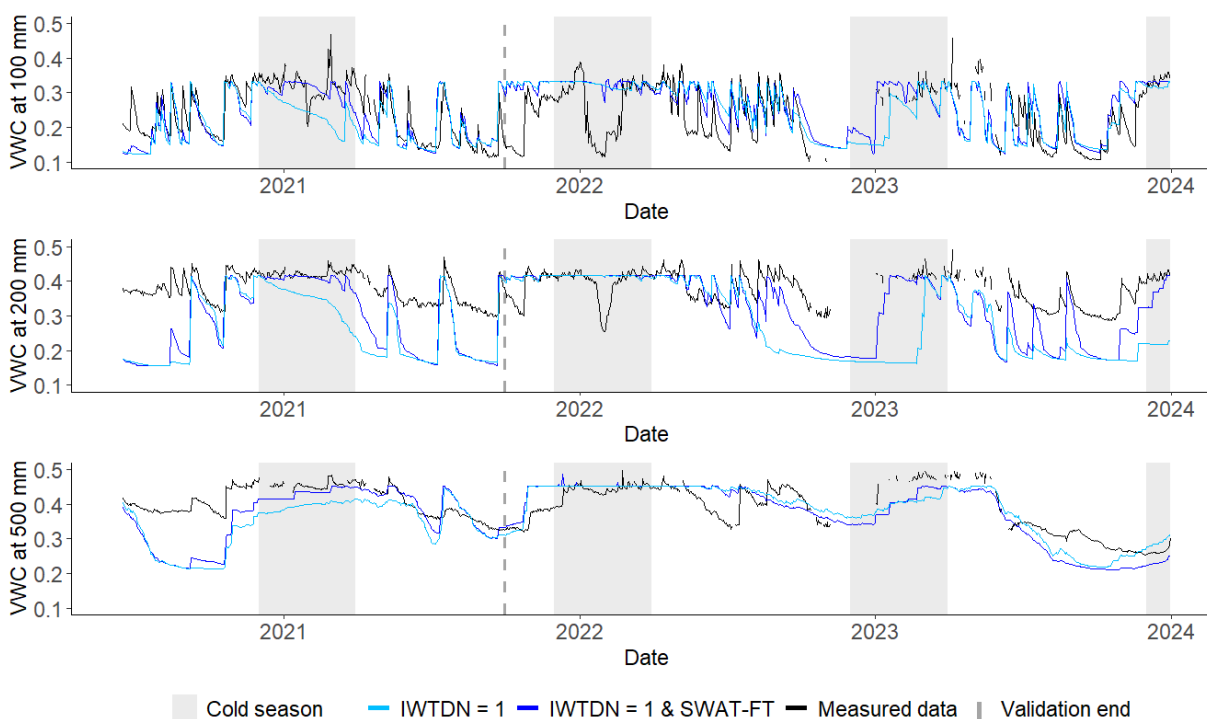


**Figure 11:** Time series of soil volumetric water content at 100 mm, 200 mm, and 500 mm from June 2020 through the end of 2023 in mm/mm. Measured data is represented by the black line, the *IWTDN=1* & *SWAT-FT* output is represented by the dark blue line, and the *IWTDN=1* output is represented by the light blue line. The validation period (ends 09/30/2021) is separated from the calibration period (starts 10/01/2021) by the vertical dashed line. Cold seasons (12/1-3/31) are highlighted in grey.

Volumetric water content at 100 mm and 200 mm do not fall within the “satisfactory” range for RSR scores, while 500 mm is within the “satisfactory” range for both executables (Table 8). The *IWTDN=1* & *SWAT-FT* executable produced a better RSR score at 200 mm depths and a similar RSR at 100 mm and 500 mm depths during the calibration period (Table 8). During the validation period, all depths improved their statistics with the addition of *SWAT-FT* (Table 8). Time series graphs show that *IWTDN=1* & *SWAT-FT* matches more peaks in the measured data during both the calibration and validation periods for volumetric water content at all three depths (the cold season in both 2020-2021 and 2022-2023) (Figure 11).

### 3.2. Evaluating improvements to the perched water table algorithm

RSR scores are mixed with addition of IWTDN=2 into the executable (Table 9). Calibration statistics show improvement for tile flow and volumetric water content at 200 mm. Other RSR values were similar between executables, except for volumetric water content at 500 mm which increased RSR (Table 9). Validation values show improvement for volumetric water content (200 mm and 500 mm) (Table 9).

**Table 9:** RSR scores comparing eight SWAT outputs across two executables. The two executables compared are (1) the *IWTDN=2 & SWAT-FT* executable (represented by the red line in figures 12-16) and (2) the *IWTDN=1 & SWAT-FT* executable (represented by the dark blue line in figures 12-16). Moriasi et al. (2007b) indicates that 0.7 and less is a satisfactory RSR at the watershed scale in a monthly time interval. Satisfactory values are in bold.

Output	Calibration		Validation		Satisfactory RSR
	IWTDN=1 & SWAT-FT	IWTDN=2 & SWAT-FT	IWTDN=1 & SWAT-FT	IWTDN=2 & SWAT-FT	
Tmp (°C) at 100 mm	<b>0.2142</b>	<b>0.2148</b>	<b>0.2760</b>	<b>0.2935</b>	< 0.7
Tmp (°C) at 200 mm	<b>0.2032</b>	<b>0.1999</b>	<b>0.2544</b>	<b>0.2718</b>	< 0.7
Tmp (°C) at 500 mm	<b>0.2784</b>	<b>0.2724</b>	<b>0.2838</b>	<b>0.2943</b>	< 0.7
Tile flow (mm)	1.0653	0.9483	1.0807	0.9869	< 0.7
Water table (mm)	0.9035	0.9460			< 0.7
VWC at 100 mm (mm/mm)	0.9473	0.9272	0.7170	0.7963	< 0.7
VWC at 200 mm (mm/mm)	1.6245	0.9972	2.8637	1.9680	< 0.7
VWC at 500 mm (mm/mm)	<b>0.6789</b>	1.2737	1.8483	1.1927	< 0.7

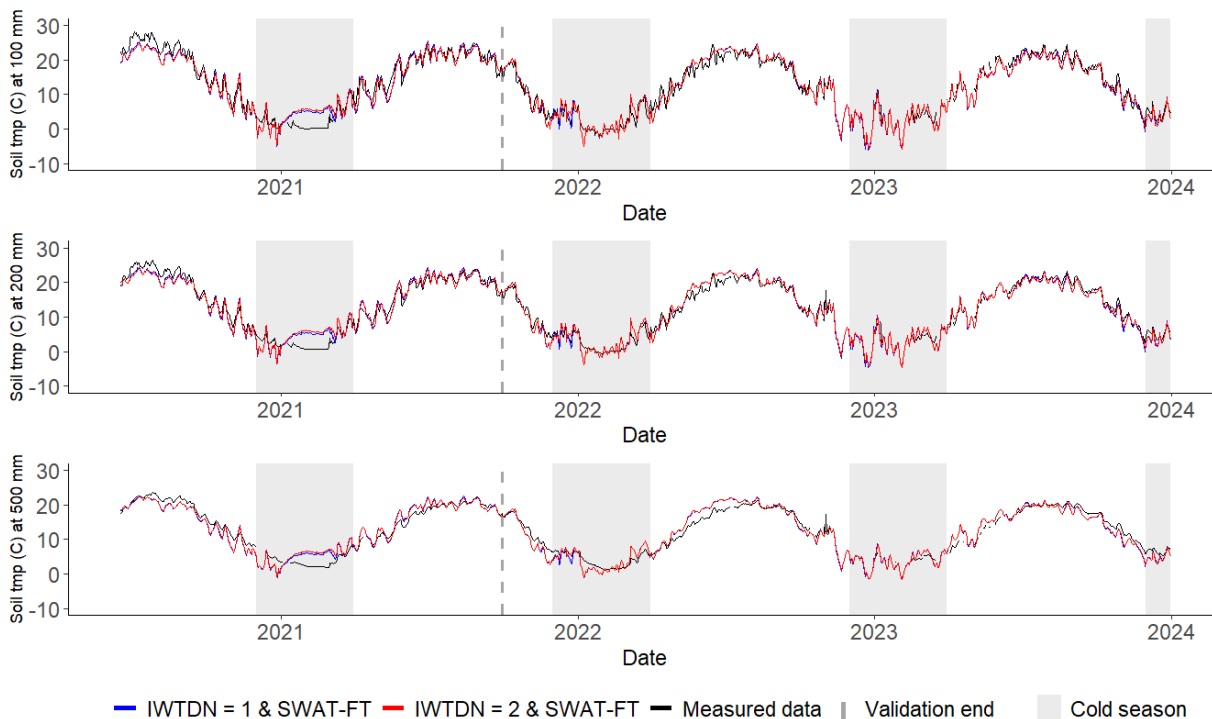


**Figure 12:** Time series of soil temperature (°C) at 100 mm, 200 mm, and 500 mm from June 2020 through the end of 2023. Measured data is represented by the black line, the *IWTDN=2 & SWAT-FT* executable is represented by the red line, and the *IWTDN=1 & SWAT-FT* executable is represented by the dark blue line. The validation period (ends 09/30/2021) is separated from the calibration period (starts 10/01/2021) by the vertical dashed line. Cold seasons (12/1-3/31) are highlighted in grey.

Both executables perform similarly across depths in simulating soil temperature (Figure 12; Table 9).

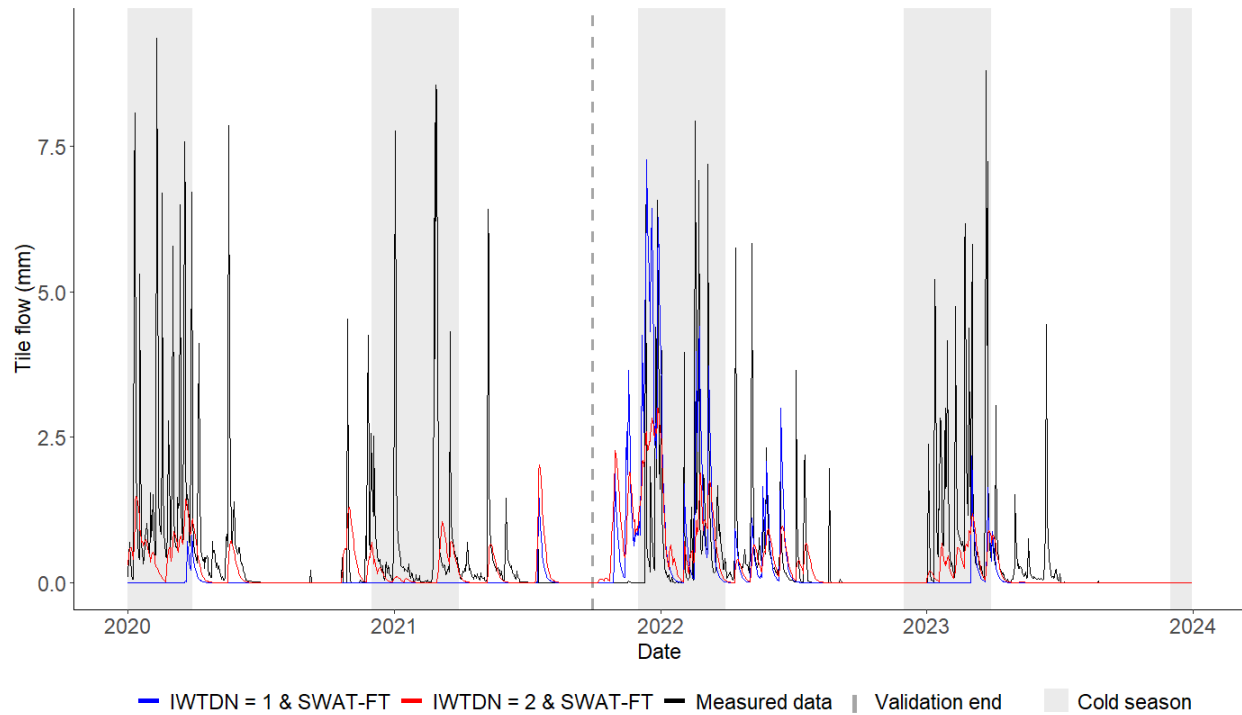


**Figure 13:** Time series of flow through the tile drains (mm) from January 2020 through the end of 2023. Measured data is represented by the black line, the *IWTDN=2 & SWAT-FT* executable is represented by the red line, and the *IWTDN=1 & SWAT-FT* executable is represented by the dark blue line. The validation period (ends 09/30/2021) is separated from the calibration period (starts 10/01/2021) by the vertical dashed line. Cold seasons (12/1-3/31) are highlighted in grey.

The *IWTDN=2 & SWAT-FT* executable shows a statistical improvement in RSR over the *IWTDN=1 & SWAT-FT* executable (Table 9). In the time series graph, the *IWTDN=2 & SWAT-FT* executable simulates more peaks in tile flow that match the measured data (mid-early 2020, 2021, late 2022, early 2023), while the *IWTDN=1 & SWAT-FT* executable does not simulate any tile flow (Figure 13). However, there are areas where the *IWTDN=2 & SWAT-FT* and *IWTDN=1 & SWAT-FT* executables over-simulate tile flow in late 2021 (Figure 13).

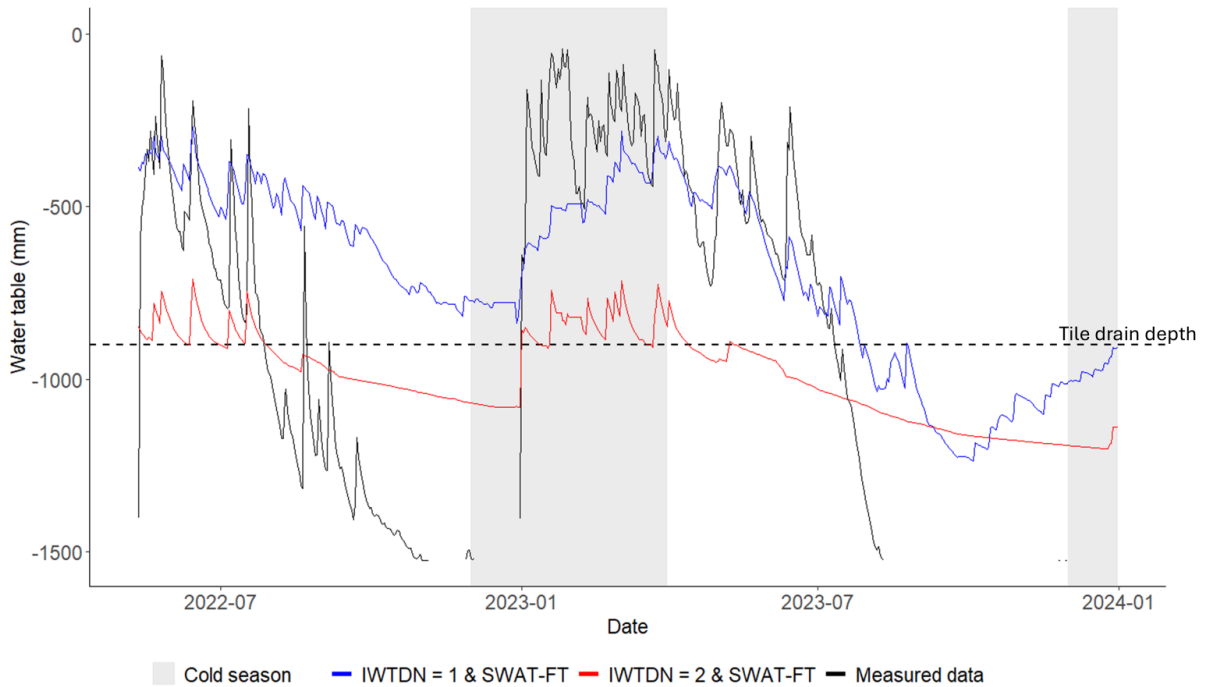


**Figure 14:** Time series of perched water table depth from the soil surface (mm) from May 2022 through the end of 2023. Measured data is represented by the black line, the *IWTDN=2 & SWAT-FT* executable is represented by the red line, and the *IWTDN=1 & SWAT-FT* executable is represented by the dark blue line. Cold seasons (12/1-3/31) are highlighted in grey.

The *IWTDN=2 & SWAT-FT* and *IWTDN=1 & SWAT-FT* executables produced similar RSR values (Table 9). In the time series graph, the *IWTDN=2 & SWAT-FT* executable is able to simulate the water table dropping to the depth of the tiles (900 mm) more often than the *IWTDN=1 & SWAT-FT* executable (Figure 14). The *IWTDN=2 & SWAT-FT* executable does not simulate the peaks in measured data close to the soil surface that the *IWTDN=1 & SWAT-FT* executable is able to reach (Figure 14). Neither executable is able to simulate the drops in water table depth to around -1500 mm (Figure 14).

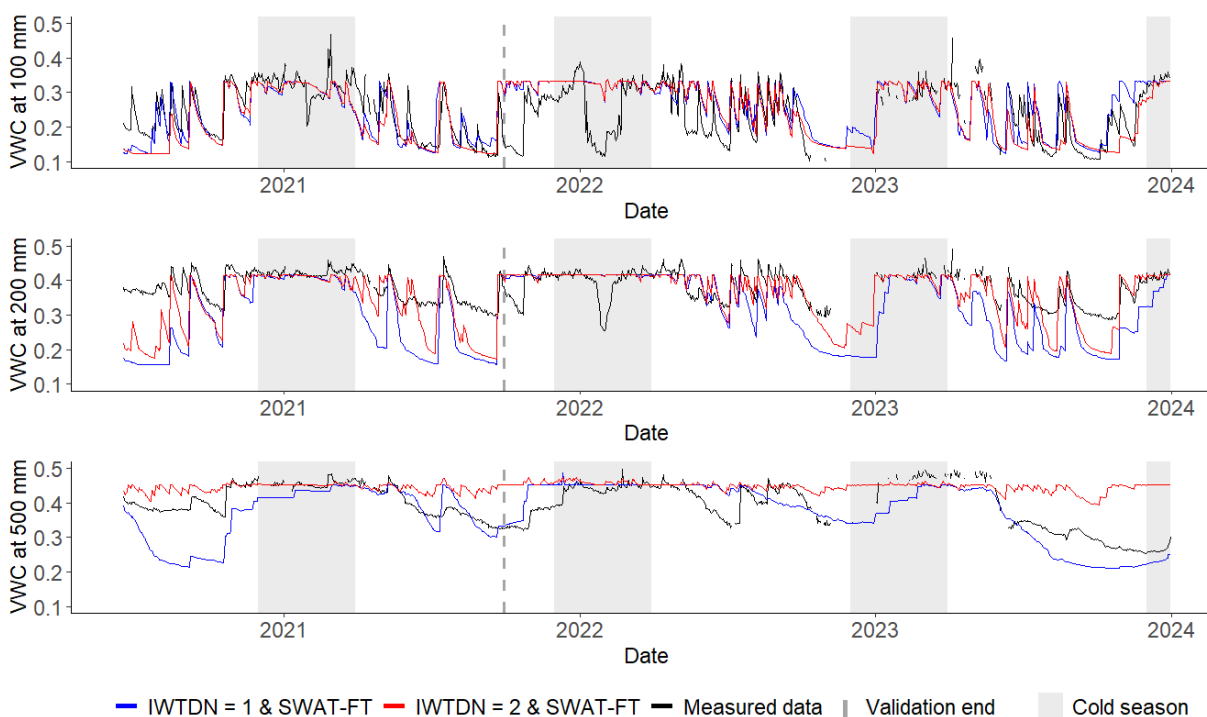


**Figure 15:** Time series of soil volumetric water content at 100 mm, 200 mm, and 500 mm from June 2020 through the end of 2023 in mm/mm. Measured data is represented by the black line, the *IWTDN=2 & SWAT-FT* executable is represented by the red line, and the *IWTDN=1 & SWAT-FT* executable is represented by the dark blue line. The validation period (ends 09/30/2021) is separated from the calibration period (starts 10/01/2021) by the vertical dashed line. Cold seasons (12/1-3/31) are highlighted in grey.

The performance of the *IWTDN=2 & SWAT-FT* executable algorithm varies across layers and depths (Table 9; Figure 15). In the 100 mm layer, the *IWTDN=1 & SWAT-FT* and *IWTDN=2 & SWAT-FT* executables produce similar RSR values (Table 9). In the 200 mm layer, the *IWTDN=1 & SWAT-FT* executable volumetric water content dips too low in comparison to the measured data (early and late 2021, late 2022, mid-late 2023) (Figure 15). The 200 mm layer RSR value performs better with the addition of *IWTDN=2* (Table 9). In the 500 mm soil layer, the *IWTDN=2 & SWAT-FT* executable stays close to where field capacity is estimated throughout the study period and performs worse statistically than *IWTDN=1 & SWAT-FT* (Figure 15; Table 9).

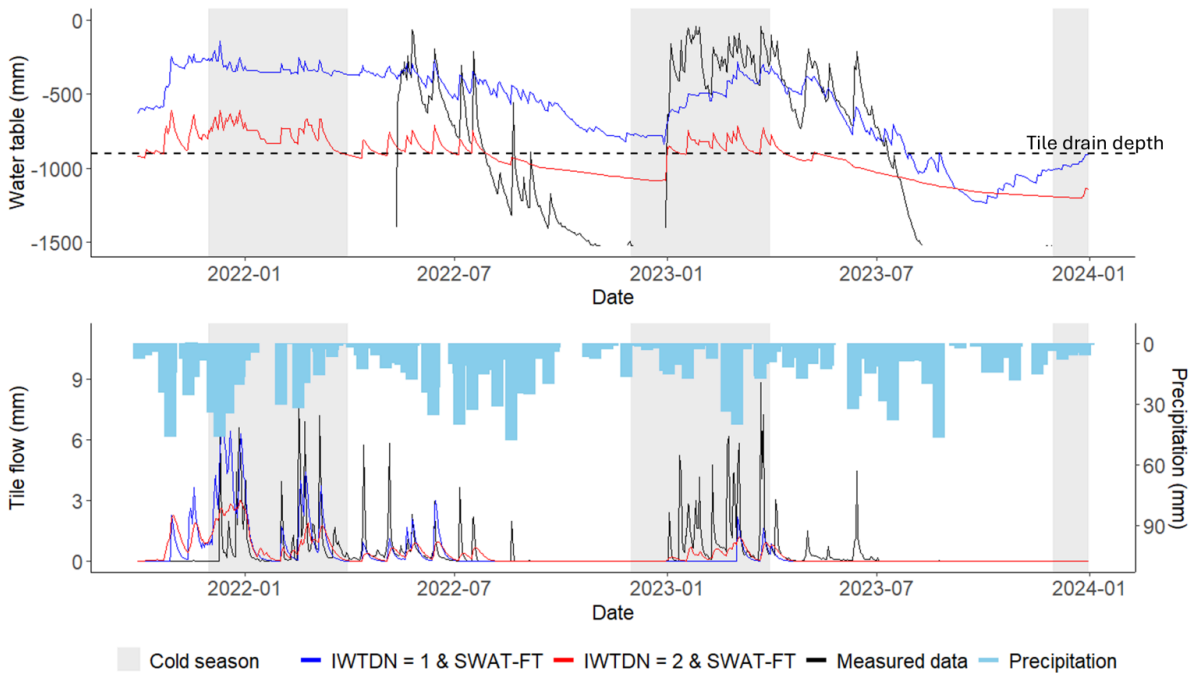


**Figure 16:** Time series of flow through the tile drains (mm), precipitation (mm), and perched water table depth (mm) during the calibration period. Measured data is represented by the black line, the SWAT output using the *IWTDN=2 & SWAT-FT* executable is represented by the red line, and the SWAT output from the *IWTDN=1 & SWAT-FT* executable is represented by the dark blue line. Cold seasons (12/1-3/31) are highlighted in grey.

Comparing the relationship between tile flow and perched water table, as the line from the *IWTDN=2 & SWAT-FT* executable rises above the tile drainage, tile flow also starts (late 2021 and late 2022-early 2023) (Figure 16). The line from the *IWTDN=1 & SWAT-FT* executable stays above the tile drains for the majority of the time period. However, the *IWTDN=1 & SWAT-FT* executable often produces no tile drainage (mid-late 2022 and early-mid 2023) (Figure 16).

### 3.3. Evaluating improvements to the perched water table algorithm without SWAT-FT

Integration of the *IWTDN=2* improvements to perched water table simulation improved statistical performance in volumetric water content at 200 mm during the calibration period, but lowered performance at 500 mm (Table 10). During the validation period, volumetric water content across all three

depths improved (Table 10). However, statistical results otherwise stayed largely the same across executable runs (Table 10).

**Table 10:** RSR scores standardized by standard deviation comparing eight SWAT outputs across two executables. The two executables compared are (1) the *IWTDN=1* executable (represented by the light blue line in figures 17-20) and (2) the *IWTDN=2* executable (represented by the green line in figures 17-20). Moriasi et al. (2007b) indicates that 0.7 and less is a satisfactory RSR at the watershed scale in a monthly time interval. Satisfactory values are in bold.

Output	Calibration		Validation		Satisfactory RSR
	IWTDN=1	IWTDN=2	IWTDN=1	IWTDN=2	
Tmp (°C) at 100 mm	<b>0.3553</b>	<b>0.3545</b>	<b>0.3471</b>	<b>0.3448</b>	< 0.7
Tmp (°C) at 200 mm	<b>0.3010</b>	<b>0.2996</b>	<b>0.3042</b>	<b>0.2993</b>	< 0.7
Tmp (°C) at 500 mm	<b>0.3312</b>	<b>0.3370</b>	<b>0.3483</b>	<b>0.3529</b>	< 0.7
Tile flow (mm)	0.9925	1.0003	1.0861	1.0550	< 0.7
Water table (mm)	1.0611	1.0366			< 0.7
VWC at 100 mm (mm/mm)	0.9732	1.0116	0.9311	0.8445	< 0.7
VWC at 200 mm (mm/mm)	2.6028	1.4081	3.2884	2.8851	< 0.7
VWC at 500 mm (mm/mm)	<b>0.6260</b>	1.2278	2.1676	0.9235	< 0.7

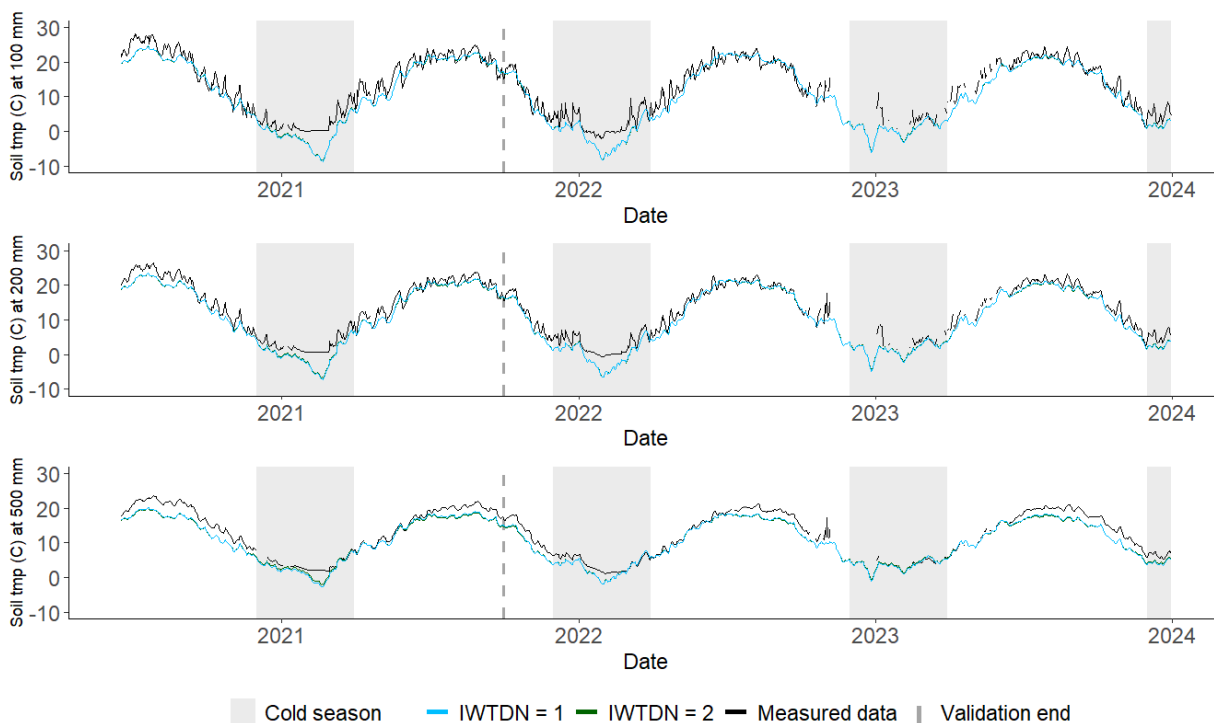


**Figure 17:** Time series of soil temperature ( $^{\circ}\text{C}$ ) at 100 mm, 200 mm, and 500 mm from June 2020 through the end of 2023. Measured data is represented by the black line, the *IWTDN=1* executable is represented by the light blue line, and the *IWTDN=2* executable is represented by the green line. The validation period (ends 09/30/2021) is separated from the calibration period (starts 10/01/2021) by the vertical dashed line. Cold seasons (12/1-3/31) are highlighted in grey.

Both executables perform similarly across depths in simulating soil temperature (Table 10; Figure 17).

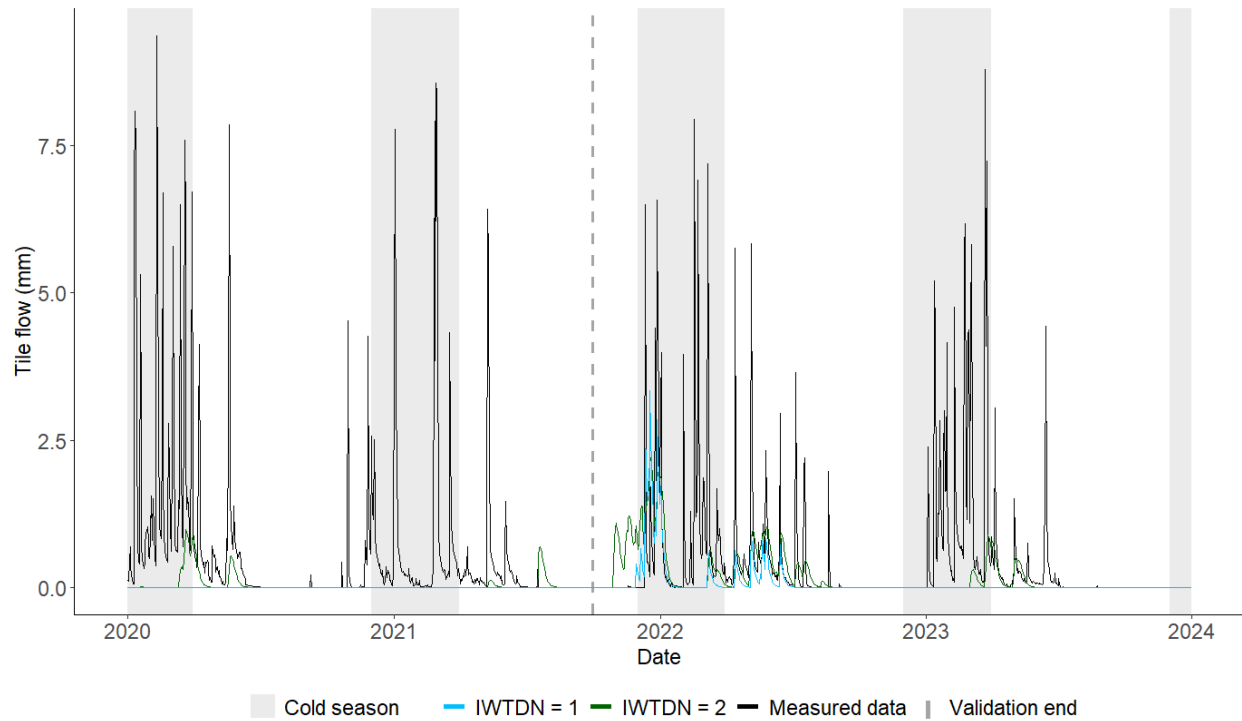


**Figure 18:** Time series of flow through the tile drains (mm) from January 2020 through the end of 2023. Measured data is represented by the black line, the *IWTDN=1* executable is represented by the light blue line, and the *IWTDN=2* executable is represented by the green line. The validation period (ends 09/30/2021) is separated from the calibration period (starts 10/01/2021) by the vertical dashed line. Cold seasons (12/1-3/31) are highlighted in grey.

In the time series graph, the *IWTDN=2* executable simulates some peaks in tile flow that match the measured data where the *IWTDN=1* executable does not simulate any tile flow (early-mid 2020, mid-late 2021, mid 2022, early-mid 2023) (Figure 18). This is consistent across the calibration and validation period (Figure 18). RSR scores do not fall within the “satisfactory” RSR score bounds and are similar between executables (Table 10).

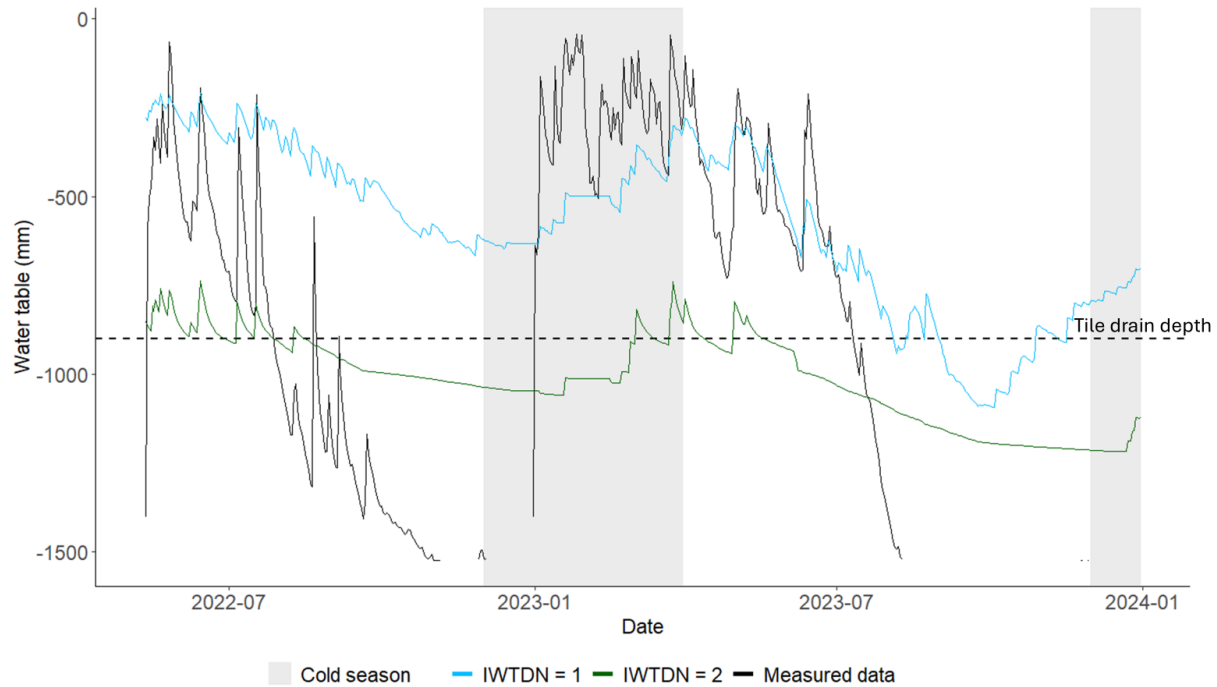


**Figure 19:** Time series of perched water table depth from the soil surface (mm) from May 2022 through the end of 2023. Measured data is represented by the black line, the *IWTDN=1* executable is represented by the light blue line, and the *IWTDN=2* executable is represented by the green line. The validation period (ends 09/30/2021) is separated from the calibration period (starts 10/01/2021) by the vertical dashed line. Cold seasons (12/1-3/31) are highlighted in grey.

The *IWTDN=2* and *IWTDN=1* executables have similar RSR performance for perched water table depth (Table 10). In the time series graph, the *IWTDN=2* executable is able to simulate the water table dropping to the depth of the tiles (900 mm) better than the *IWTDN=1* executable (Figure 19). The *IWTDN=2* executable does not simulate the peaks in measured data close to the soil surface that the *IWTDN=1* executable is able to reach (Figure 19). Neither executable is able to reach the drops in perched water table depth to around -1500 mm (Figure 19).

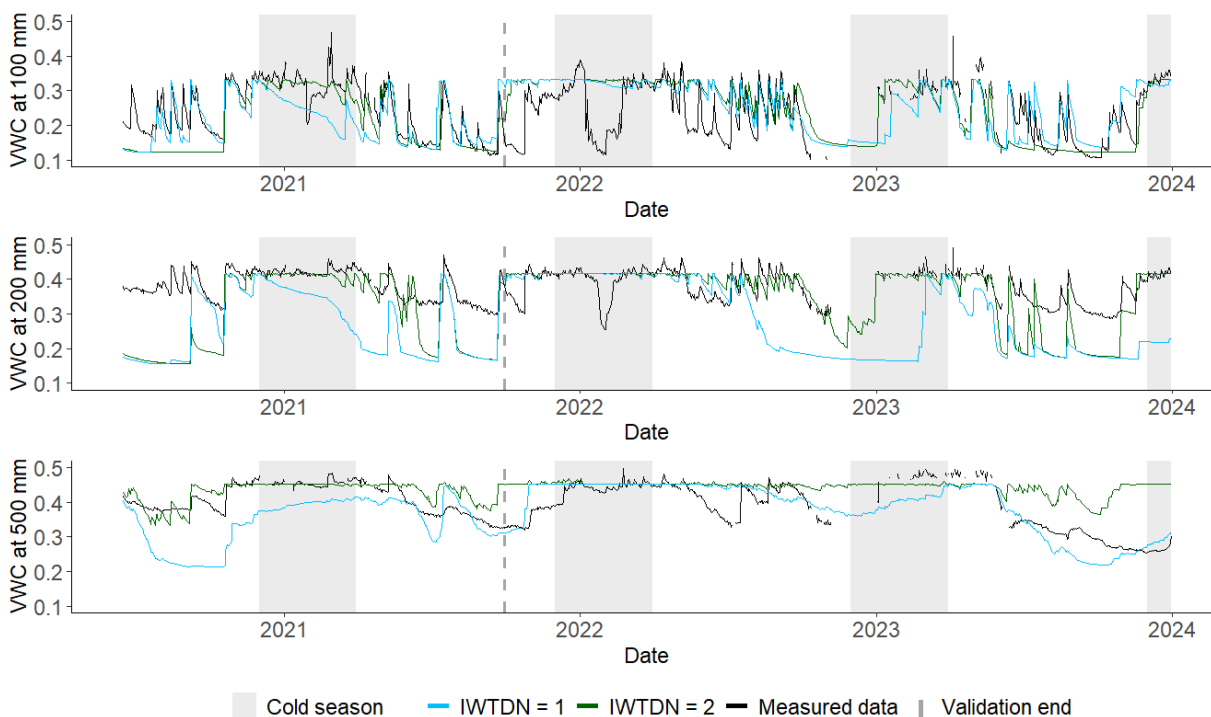


**Figure 20:** Time series of soil volumetric water content at 100 mm, 200 mm, and 500 mm from June 2020 through the end of 2023 in mm/mm. Measured data is represented by the black line, the *IWTDN=1* executable is represented by the light blue line, and the *IWTDN=2* executable is represented by the green line. The validation period (ends 09/30/2021) is separated from the calibration period (starts 10/01/2021) by the vertical dashed line. Cold seasons (12/1-3/31) are highlighted in grey.

The performance of the *IWTDN=2* executable improvements vary across layers and depths (Table 10; Figure 20). In all layers, the *IWTDN=1* executable dips below the measured data more often than *IWTDN=2* in both the calibration and validation periods (2020, 2021, mid 2022-early 2023) (Figure 20). However, in the 100 mm and 500 mm layers, the *IWTDN=1* executable is able to more closely match the dip in soil water towards the end of 2023 (Figure 20). In the 500 mm soil layer, the *IWTDN=2* executable stays close to where field capacity is estimated throughout the study period and performs worse statistically than *IWTDN=1* (Figure 20; Table 10).

KGE, NSE, PBIAS, and  $R^2$  statistics can be found in the Appendix (8-11). These statistics were not used in model calibration.

### 3.4. Cold season results

The executables that contain SWAT-FT are able to simulate soil temperature at 100 mm and 200 mm during cold seasons (12/1-3/31) with a satisfactory RSR during the calibration period (Table 11). Results for RSR statistics during the cold seasons within the validation period were more mixed (Table 12).

**Table 11:** RSR statistics for only the cold seasons (12/1-3/31) during the calibration period for each executable (Table 6). The model was not calibrated to these metrics. Moriasi et al. (2007b) indicates that 0.7 and less is a satisfactory RSR at the watershed scale in a monthly time interval. Satisfactory values are in bold.

Calibration time period					
Output	IWTDN=1	IWTDN=1 & SWAT-FT	IWTDN=2	IWTDN=2 & SWAT-FT	Satisfactory RSR
Tmp (°C) at 100 mm	1.2944	<b>0.6222</b>	1.2873	<b>0.6205</b>	< 0.7
Tmp (°C) at 200 mm	1.2284	<b>0.6916</b>	1.2094	<b>0.6763</b>	< 0.7
Tmp (°C) at 500 mm	0.8524	0.8832	0.8016	0.8691	< 0.7
Tile flow (mm)	1.0767	1.1313	1.0806	0.9747	< 0.7
Water table (mm)	1.0062	0.9325	2.2970	1.8830	< 0.7
VWC at 100 mm (mm/mm)	1.1998	1.1352	1.1796	1.1386	< 0.7
VWC at 200 mm (mm/mm)	3.3995	1.3951	1.0468	1.0459	< 0.7
VWC at 500 mm (mm/mm)	<b>0.5185</b>	<b>0.4627</b>	1.0887	1.0940	< 0.7

**Table 12:** RSR statistics for only the cold seasons (12/1-3/31) during the validation period for each executable (Table 6). Moriasi et al. (2007b) indicates that 0.7 and less is a satisfactory RSR at the watershed scale in a monthly time interval. Satisfactory values are in bold.

Validation time period					
Output	IWTDN=1	IWTDN=1 & SWAT-FT	IWTDN=2	IWTDN=2 & SWAT-FT	Satisfactory RSR
Tmp (°C) at 100 mm	1.4790	1.1664	1.4490	1.2772	< 0.7
Tmp (°C) at 200 mm	1.5457	1.3647	1.4700	1.4975	< 0.7
Tmp (°C) at 500 mm	1.2473	1.7498	1.0156	1.9373	< 0.7
Tile flow (mm)	1.1870	1.1768	1.1558	1.0655	< 0.7
VWC at 100 mm (mm/mm)	2.5217	1.2910	1.1497	1.2396	< 0.7
VWC at 200 mm (mm/mm)	8.4359	2.4253	1.8717	2.0005	< 0.7
VWC at 500 mm (mm/mm)	4.1651	1.9704	1.0837	1.0444	< 0.7

## 4. Discussion and future work

### 4.1. The single field model

SWAT was built for watershed scale hydrology simulation, often with hundreds of sub-units (called HRUs), where model output outliers and trends are smoothed out across HRUs. This is similar to how an average can gloss over outliers. A single-field SWAT model allows researchers to test source code modifications on a scale where the effect of algorithm adjustments is more clear and allows the analysis of field-scale processes. Looking at model outputs on the field-scale highlights where there is further room for improvement within the model.

Comparing measured data to SWAT outputs at the field-scale allows for close examination of field-level processes. Calibration becomes difficult if the model simulation location and the sampling location of the measured data are different. For example, the volumetric water content measurement was taken closer to the edge of the field, but SWAT simulates volumetric water uniformly across the field. Also, perched water table depth measurements were taken between the tile drains where the water table would be the closest to the soil surface during wet conditions, but SWAT simulates perched water table as an average across the field. It is important to note that measured data is often difficult to replicate using single-field model outputs. This should be considered as a limitation when analyzing model results

### 4.2. Soil temperature outputs

The model executable with improvements to heat transfer in the soil profile (SWAT-FT) (Qi et al., 2016a,b; 2019) produced results that are always statistically satisfactory over the whole study period (Table 8). During the winter, the executables with SWAT-FT produced soil temperature outputs that align more closely with measured data, particularly at more shallow depths (100 mm and 200 mm) (Table 8, Table 11, Figure 8). The model was calibrated to year round data, not just the cold season. Therefore, it is worth noting that cold season statistics for soil temperature improve at 100 mm and 200 mm depths. Results for soil temperature were similar for comparisons between model executables that had the same

SWAT-FT flag (i.e. both had the SWAT-FT flag turned off or both had the SWAT-FT flag turned on) (Figure 12 and 17), which is expected since the temperature routines are the same. The SWAT-FT method shows improvement in soil temperature simulation when calibrated in Ohio, showing that soil temperature algorithm improvements should be added to the SWAT model, especially for regions with cold seasons.

Previous studies that looked at the SWAT-FT source code improvements generally found that the SWAT-FT improved soil temperature simulation (Qi et al., 2016a,b;2019). Qi et al. (2016a,b) performed two studies in New Brunswick, Canada that found improvement in soil temperature simulation with SWAT-FT, especially at deeper depths. Both studies highlighted that soil temperature inconsistencies could be attributed to inaccurate estimation of snow depth within the SWAT model, which could be important for future work. Qi et al. (2019) also did a study in the Upper Mississippi River Basin (Minnesota, Wisconsin, Iowa, Illinois, Missouri) that found that soil temperature simulation was improved with SWAT-FT, especially at deeper layers, as well. In contrast, the calibration results from this thesis also saw improvements in soil temperature simulation, but especially during the cold season at more shallow depths (Table 8 and Table 11). The difference in performance by depth could be due to different model parameters.

The SWAT-FT method (Qi et al., 2016a,b; 2019) is also an important update to integrate into SWAT for projects that include hydrology outputs. Executables that include SWAT-FT improved the simulation of volumetric water content in many areas, especially during the validation period (Table 8; Figure 11). During the cold season, executables with SWAT-FT saw some improvement in perched water table simulation and volumetric water content at especially 200 mm and 500 mm when comparing  $IWTDN=1$  to  $IWTDN=1$  & *SWAT-FT* (Table 11). The improvement of subsurface hydrology outputs shows that better simulation of the soil profile temperature is crucial for water movement in SWAT.

### 4.3. Hydrology outputs

The SWAT hydrology outputs did not always improve statistically with IWTDN=2. This is not unexpected since a constraint was added to the model by coupling soil moisture with perched water table simulation. A constraint on the model can limit model performance, and because perched water table is also tied to tile drain flow, all of the hydrology outputs are affected. However, IWTDN=2 made the simulation of the perched water table more physically based and realistic. The Moriasi et al. (2011) approach (executables with IWTDN =1) initializes the perched water table depth at the beginning of the simulation period and then adjusts it daily based on the change in soil water content multiplied by an adjustment factor. IWTDN=1 is only initialized once, which causes the water table to creep around and can lead to situations where perched water table depth, soil moisture, and tile drainage are disconnected. The disconnect is shown when IWTDN=1 simulates a high perched water but there is no tile flow (Figure 16). IWTDN=2 initializes the calculation of water table depth every day by calculating the excess soil moisture in each soil layer. Tile drainage simulated by IWTDN=2 corresponds to a rise in the perched water table above the tile drains, showing that perched water table, soil moisture, and tile flow are more connected and realistic (Figure 16). Further work will be needed to improve the perched water table's statistical performance, but the approach outlined in this thesis is a step towards making the algorithm more physically based. The lack of improvement in statistical performance with IWTDN=2 was likely due to the model constraint. Future work could consider adding a penalty factor to IWTDN=1 statistics to account for unrealistic behavior.

Connecting soil water, tile flow, and perched water table depth in IWTDN=2 was the first step in improving the perched water table depth simulation. Further improvements are needed to allow the perched water table depth to rise and fall as quickly and dramatically as the measured data. IWTDN=2 was unable to reach the more shallow measured data peaks near the soil surface. In the field, the perched water table is curved (Yousfi et al., 2014), deeper near the tile drains and more shallow in between the tiles, while SWAT simulates the perched water table as a flat line. The measured water table data was

taken between the tile drains where the water table would be curved towards the soil surface, which may contribute to why IWTDN=2 was unable to reach the more shallow measured data peaks closer to the soil surface. IWTDN=2 is also unable to get deep enough to match measured data dips. The lack of depth warrants further exploration of how SWAT handles the water balance. IWTDN=2 may not be capturing lateral flow, evapotranspiration, or deep percolation, which allow water to leave the perched water table.

The calculation of perched water table for IWTDN=2 also assumes that the soil would be saturated between the impervious layer and the top of the perched water table. However, since the perched water table curves towards the soil surface between the tile drains in the field, the average perched water table depth that SWAT calculates has air in the pore space as well as water. To account for SWAT simulating a flat perched water table depth, future work could incorporate the volume of air in the pore space above field capacity ( $V_{air}$ ) into the perched water table algorithm. SWAT-M and SWAT2009 (Appendix 2-3) included  $V_{air}$  in water table calculations, but kept the value stationary at  $V_{air} = 0.5$ . A large  $V_{air}$  led to a small denominator in the SWAT-M and SWAT2009 calculations, which created an unrealistically high water table without adjustments. Future work should integrate a smaller, variable  $V_{air}$  to improve the speed of water table change while still producing reasonable values.

Water table initialization point should be looked into further. IWTDN=2 initializes the water table at the bottom of the SWAT soil profile, or the depth to impervious layer, whichever is more shallow. However, there are situations where the depth to the impervious layer is below the bottom of the SWAT soil profile. The decision to initialize the water table at whichever depth was more shallow was made because it is not clear which soil characteristics exist below the bottom of the profile, and therefore it is hard to know if the behavior of soil water is logical. Future work should explore ways to initialize the water table depth below the bottom of the SWAT soil profile to be able to handle these scenarios.

The depth to the impervious layer is also a factor to consider in future model improvements. The depth of the impervious layer not only controls the location of the perched water table, but also the permeability of the impervious layer (Frankenberger, 2014). As the depth to the impervious layer moves deeper in the soil profile, the seepage factor increases, allowing more water through the impervious layer. Future work needs to separate the depth to the impervious layer from the permeability of the impervious layer.

Tile flow was improved by  $IWTDN=2$ . Simulated data with  $IWTDN=2$  matches more tile flow peaks and is statistically better during the calibration period (Figure 13; Table 9). Calibrating to measured volumetric water content is a novel approach. The improvements to the simulation of volumetric water content when compared to measured data are mixed (Table 8-10). The three layers simulated responded differently to changes in the calibration parameters, which adds complexity to model parameters (Table 8-10; Figure 11, Figure 15, Figure 20). However, calibrating to soil moisture introduces a new insight into the SWAT model, allowing the opportunity to examine in-field hydrology dynamics.

#### 4.4. Calibration

This model calibration focused on eight SWAT outputs that all have different responses to changes in parameters. Highly dimensional calibration with many parameters is complex because a parameter adjustment might increase the accuracy of one SWAT output and decrease the performance of a different output. In the future, complex calibration problems could benefit from a more robust calibration approach that finds the optimal set of parameters rather than relying on a random combination of parameters finding the best possible parameter set. Future calibration approaches could weight important outputs higher. The 500 mm layers for soil temperature and volumetric water content may be most important since they have the least interference from the soil surface and therefore could be weighted higher during calibration. Future calibration approaches should also include a more complex calibration of bulk density, available water content, and soil composition because these variables are used by SWAT to calculate saturation, field capacity, and wilting point.

It is also important to note that the calibration method used in this thesis relies on a random combination of parameters within a set range being the best fit. Future work should include a more detailed and exhaustive approach to calibration. The Kalcic Lab is collaborating with a research team at the Ohio State University to develop a more robust machine learning based calibration approach. Machine learning and derivative-free optimization methods are promising for future calibration of high-dimensional models (Scyphers et al., 2024).

## 5. Conclusion

A SWAT model of a field in Hardin county, Ohio was used to test source code modifications to soil temperature (Qi et al., 2016a,b; 2019) and perched water table depth calculations. A calibration approach was developed using SWATrunR to analyze results from novel algorithms in SWAT.

The SWAT model improvements to soil temperature and perched water depth calculations should also be made in SWAT+. The SWAT2012 limitations this thesis addresses in soil temperature and perched water table depth simulation also apply to the SWAT+ source code (SWAT+ source code version 61.0.2).

This thesis found the following results:

- A single-field SWAT model proved a useful tool to analyze field-level processes and closely examine how source code changes affect model outputs in SWAT, especially paired with extensive field monitoring data.
- Integration of the Qi et al. (2016a,b; 2019) source code changes to soil temperature calculation improved soil temperature simulation across all depths (100 mm, 200 mm, and 500 mm). During the cold season, 100 mm and 200 mm depths particularly improved.
- Improvements to the calculation of the perched water table depth more closely coupled the water table to soil moisture, making for more physically meaningful simulation of the water table, yet the additional constraint did not result in improved calibration statistics of water table against measured data.
- Integration of both the water table and soil temperature improvements generated better performance statistics for tile flow and volumetric water content at 200 mm during the calibration period.
- Comprehensive calibration and sensitivity analysis would allow further detection of structural strengths and weaknesses within the SWAT model.

## References

- Apostel, A., Kalcic, M., Dagnew, A., Evenson, G., Kast, J., King, K., Martin, J., Muenich, R. L., & Scavia, D. (2021). Simulating internal watershed processes using multiple SWAT models. *Science of The Total Environment*, 759, 143920. <https://doi.org/10.1016/j.scitotenv.2020.143920>
- Arnold, J. G., Srinivasan, R., Muttiah, R. S., & Williams, J. R. (1998). Large area hydrologic modeling and assessment part I: model development 1. *JAWRA Journal of the American Water Resources Association*, 34(1), 73-89.
- Bosch, N. S., Evans, M. A., Scavia, D., & Allan, J. D. (2014). Interacting effects of climate change and agricultural BMPs on nutrient runoff entering Lake Erie. *Journal of Great Lakes Research*, 40(3), 581–589. <https://doi.org/10.1016/j.jglr.2014.04.011>
- Chaffin, J. D., Kane, D. D., Stanislawczyk, K., & Parker, E. M. (2018). Accuracy of data buoys for measurement of cyanobacteria, chlorophyll, and turbidity in a large lake (Lake Erie, North America): Implications for estimation of cyanobacterial bloom parameters from water quality sonde measurements. *Environmental Science and Pollution Research*, 25(25), 25175–25189. <https://doi.org/10.1007/s11356-018-2612-z>
- Chu, T. W., and A. Shirmohammadi. (2004). Evaluation of the SWAT model's hydrology component in the piedmont physiographic region of Maryland. *Trans. ASAE* 47(4): 1057-1073.
- CropScape—Cropland Data Layer, years 2022 at 30-meter resolution (2022), <https://nassgeodata.gmu.edu/CropScape/>.
- Culman, S., Mann, M., Sharma, S., Saeed, M., Fulford, A., Lindsey, L., ... & Joern, B. (2019). Converting between Mehlich-3, Bray P, and ammonium acetate soil test values. *The Ohio State University, College of Food, Agricultural, and Environmental Sciences. Fact Sheet: ANR-75*.
- Dahl, T. E. (1990). Wetlands losses in the United States, 1780's to 1980's. *US Department of the Interior, Fish and Wildlife Service*.

- Darzi-Naftchali, A., Mirlatifi, S. M., Shahnazari, A., Ejlali, F., & Mahdian, M. H. (2013). Effect of subsurface drainage on water balance and water table in poorly drained paddy fields. *Agricultural Water Management*, *130*, 61–68. <https://doi.org/10.1016/j.agwat.2013.08.017>
- Dodds, W. K., Bouska, W. W., Eitzmann, J. L., Pilger, T. J., Pitts, K. L., Riley, A. J., Schloesser, J. T., & Thornbrugh, D. J. (2009). Eutrophication of U.S. Freshwaters: Analysis of Potential Economic Damages. *Environmental Science & Technology*, *43*(1), 12–19. <https://doi.org/10.1021/es801217q>
- Doran, J. W., & Zeiss, M. R. (2000). Soil health and sustainability: Managing the biotic component of soil quality. *Applied Soil Ecology*, *15*(1), 3–11. [https://doi.org/10.1016/S0929-1393\(00\)00067-6](https://doi.org/10.1016/S0929-1393(00)00067-6)
- Douglas-Mankin, K. R., Srinivasan, R., & Arnold, J. G. (2010). Soil and Water Assessment Tool (SWAT) model: Current developments and applications. *Transactions of the ASABE*, *53*(5), 1423-1431.
- Du, B., Arnold, J. G., Saleh, A., & Jaynes, D. B. (2005). Development and application of SWAT to landscapes with tiles and potholes. *Transactions of the ASAE*, *48*(3), 1121–1133. <https://doi.org/10.13031/2013.18522>
- Duncan, E. W., King, K. W., Williams, M. R., LaBarge, G., Pease, L. A., Smith, D. R., & Fausey, N. R. (2017). Linking Soil Phosphorus to Dissolved Phosphorus Losses in the Midwest. *Agricultural & Environmental Letters*, *2*(1), 170004. <https://doi.org/10.2134/ael2017.02.0004>
- Engman, E. T. (1986). Roughness Coefficients for Routing Surface Runoff. *Journal of Irrigation and Drainage Engineering*, *112*(1), 39–53. [https://doi.org/10.1061/\(ASCE\)0733-9437\(1986\)112:1\(39\)](https://doi.org/10.1061/(ASCE)0733-9437(1986)112:1(39))
- Fouss, J. L. (1973). Structural design procedure for corrugated plastic drainage tubing (No. 1466). *US Department of Agriculture*.
- Frankenberger, J. (2014). *Great Lakes SWAT Conference proceedings*. [https://graham.umich.edu/media/files/watercenter/Frankenberger\\_Tile-drainage-in-SWAT.pdf](https://graham.umich.edu/media/files/watercenter/Frankenberger_Tile-drainage-in-SWAT.pdf)

- Gray, D. M., & Landine, P. G. (1988). An energy-budget snowmelt model for the Canadian Prairies. *Canadian Journal of Earth Sciences*, 25(8), 1292–1303. <https://doi.org/10.1139/e88-124>
- Hanrahan, B. R., King, K. W., Williams, M. R., Duncan, E. W., Pease, L. A., & LaBarge, G. A. (2019). Nutrient balances influence hydrologic losses of nitrogen and phosphorus across agricultural fields in northwestern Ohio. *Nutrient Cycling in Agroecosystems*, 113(3), 231–245. <https://doi.org/10.1007/s10705-019-09981-4>
- Jaynes, D. B., & James, D. E. (2007). The extent of farm drainage in the United States. *US Department of Agriculture*.
- Kahlowan, M. A., Ashraf, M., & Zia-ul-Haq. (2005). Effect of shallow groundwater table on crop water requirements and crop yields. *Agricultural Water Management*, 76(1), 24–35. <https://doi.org/10.1016/j.agwat.2005.01.005>
- Kalcic, M. M., Kirchoff, C., Bosch, N., Muenich, R. L., Murray, M., Griffith Gardner, J., & Scavia, D. (2016). Engaging Stakeholders To Define Feasible and Desirable Agricultural Conservation in Western Lake Erie Watersheds. *Environmental Science & Technology*, 50(15), 8135–8145. <https://doi.org/10.1021/acs.est.6b01420>
- Kerr, J. M., DePinto, J. V., McGrath, D., Sowa, S. P., & Swinton, S. M. (2016). Sustainable management of Great Lakes watersheds dominated by agricultural land use. *Journal of Great Lakes Research*, 42(6), 1252–1259. <https://doi.org/10.1016/j.jglr.2016.10.001>
- King, K. W., Fausey, N. R., & Williams, M. R. (2014). Effect of subsurface drainage on streamflow in an agricultural headwater watershed. *Journal of Hydrology*, 519, 438–445. <https://doi.org/10.1016/j.jhydrol.2014.07.035>
- King, K. W., Williams, M. R., LaBarge, G. A., Smith, D. R., Reutter, J. M., Duncan, E. W., & Pease, L. A. (2018). Addressing agricultural phosphorus loss in artificially drained landscapes with 4R nutrient management practices. *Journal of Soil and Water Conservation*, 73(1), 35–47. <https://doi.org/10.2489/jswc.73.1.35>

- Kladivko, E. J., & Bowling, L. C. (2021). Long-term impacts of drain spacing, crop management, and weather on nitrate leaching to subsurface drains. *Journal of Environmental Quality*, 50(3), 627–638. <https://doi.org/10.1002/jeq2.20215>
- Kladivko, E. J., Frankenberger, J. R., Jaynes, D. B., Meek, D. W., Jenkinson, B. J., & Fausey, N. R. (2004). Nitrate Leaching to Subsurface Drains as Affected by Drain Spacing and Changes in Crop Production System. *Journal of Environmental Quality*, 33(5), 1803–1813. <https://doi.org/10.2134/jeq2004.1803>
- Kleinman, P. J. A., Smith, D. R., Bolster, C. H., & Easton, Z. M. (2015). Phosphorus Fate, Management, and Modeling in Artificially Drained Systems. *Journal of Environmental Quality*, 44(2), 460–466. <https://doi.org/10.2134/jeq2015.02.0090>
- Knoben, W. J. M., Freer, J. E., & Woods, R. A. (2019). Technical note: Inherent benchmark or not? Comparing Nash–Sutcliffe and Kling–Gupta efficiency scores. *Hydrology and Earth System Sciences*, 23(10), 4323–4331. <https://doi.org/10.5194/hess-23-4323-2019>
- Li, Q., Qi, J., Xing, Z., Li, S., Jiang, Y., Danielescu, S., Zhu, H., Wei, X., & Meng, F.-R. (2014). An approach for assessing impact of land use and biophysical conditions across landscape on recharge rate and nitrogen loading of groundwater. *Agriculture, Ecosystems & Environment*, 196, 114–124. <https://doi.org/10.1016/j.agee.2014.06.028>
- Madramootoo, C. A., Johnston, W. R., Ayars, J. E., Evans, R. O., & Fausey, N. R. (2007). Agricultural drainage management, quality and disposal issues in North America. *Irrigation and Drainage*, 56(S1), S35–S45. <https://doi.org/10.1002/ird.343>
- Monke, E. J., Huggins, L. F., Galloway, H. M., & Foster, G. R. (1967). Field study of subsurface drainage on a slowly permeable soil. *Transactions of the ASAE*, 10(4), 573-0576.
- Moriasi, D. N., Arnold, J. G., & Green, C. H. (2007a). Incorporation of Hooghoudt and Kirkham tile drain equations into SWAT2005. *In Proc. 4th Intl. SWAT Conf UNESCO-IHE Delft, The Netherlands*. 139-147.

- Moriasi, D. N., Arnold, J. G., Van Liew, M. W., Bingner R. L., Harmel, R. D., & Veith., T. L. (2007b). Model Evaluation Guidelines for Systematic Quantification of Accuracy in Watershed Simulations. *Transactions of the ASABE*, 50(3), 885–900. <https://doi.org/10.13031/2013.23153>
- Moriasi, D. N., Arnold, J. G., Vazquez-Amábile, G. G., Engel., B. A & Rossi., C. G. (2009). Incorporation of a New Shallow Water Table Depth Algorithm into SWAT2005. *Transactions of the ASABE*, 52(3), 771–784. <https://doi.org/10.13031/2013.27398>
- Moriasi, D. N., Arnold, J. G., Vazquez-Amábile, G. G., & Engel., B. A. (2011). Shallow Water Table Depth Algorithm in SWAT: Recent Developments. *Transactions of the ASABE*, 54(5), 1705–1711. <https://doi.org/10.13031/2013.39850>
- Moriasi, D. N., Rossi, C. G., Arnold, J. G., & Tomer, M. D. (2012). Evaluating hydrology of the Soil and Water Assessment Tool (SWAT) with new tile drain equations. *Journal of Soil and Water Conservation*, 67(6), 513–524. <https://doi.org/10.2489/jswc.67.6.513>
- Moriasi, D. (2015). Hydrologic and Water Quality Models: Performance Measures and Evaluation Criteria. *Transactions of the ASABE*, 58(6), 1763–1785. <https://doi.org/10.13031/trans.58.10715>
- Morse, H. H., & Bone, S. (1958). *Understanding Ohio Soils*.
- Mourtzinis, S., Andrade, J. F., Grassini, P., Edreira, J. I. R., Kandel, H., Naeve, S., Nelson, K. A., Helmers, M., & Conley, S. P. (2021). Assessing benefits of artificial drainage on soybean yield in the North Central US region. *Agricultural Water Management*, 243, 106425. <https://doi.org/10.1016/j.agwat.2020.106425>
- Natural Resources Conservation Service. (2008). *Soil Quality Indicators*. [https://www.nrcs.usda.gov/sites/default/files/2022-10/nrcs142p2\\_051591.pdf#:~:text=Bulk%20density%20typically%20increases%20with%20soil%20depth,compacting%20weight%20of%20the%20soil%20above%20them](https://www.nrcs.usda.gov/sites/default/files/2022-10/nrcs142p2_051591.pdf#:~:text=Bulk%20density%20typically%20increases%20with%20soil%20depth,compacting%20weight%20of%20the%20soil%20above%20them).
- Nietch, C., Gledhill, P., Smucker, N., Heberling, M., Pilgrim. E., Mitchell, R., Pollard A., & Yuan, L., (2023). How Small Stream Monitoring and a Benthic Algae DNA Metabarcoding Study has Informed TMDL Development in a SW Ohio Watershed. *NALMS LAKELINE*.

- Neitsch S., Arnold, J., Kiniry, J. R., Williams, J. R., & King, K. W. (2000). *Soil and Water Assessment Tool Theoretical Documentation*.  
<https://swat.tamu.edu/media/1290/swat2000theory.pdf>
- Neitsch S., Arnold, J., Kiniry, J. R., & Williams, J. R. (2005). *Soil and Water Assessment Tool Theoretical Documentation*. <https://swat.tamu.edu/media/1292/swat2005theory.pdf>
- Neitsch S., Arnold, J., Kiniry, J. R., & Williams, J. R. (2009). *Soil and Water Assessment Tool Theoretical Documentation*. <https://swat.tamu.edu/media/1292/swat2005theory.pdf>
- NOAA-NCEI (2019). National Oceanic and Atmospheric Administration, Station:USC00330563, BELLEFONTAINE, OH US. Date Accessed: July 2023.  
<https://www.ncei.noaa.gov/access/past-weather/40.651417,-83.791048,40.151417,-83.291048>
- Ohio P Task Force (OLEPTF). (2013). Ohio P Task Force II final report. *Ohio Department of Agriculture, Ohio Department of Natural Resources, Ohio Environmental Protection Agency, and Ohio Lake Erie Commission*.
- Osterholz, W. R., Hanrahan, B. R., & King, K. W. (2020). Legacy phosphorus concentration–discharge relationships in surface runoff and tile drainage from Ohio crop fields. *Journal of Environmental Quality*, 49(3), 675–687. <https://doi.org/10.1002/jeq2.20070>
- Paerl, H. W., Scott, J. T., McCarthy, M. J., Newell, S. E., Gardner, W. S., Havens, K. E., Hoffman, D. K., Wilhelm, S. W., & Wurtsbaugh, W. A. (2016). It Takes Two to Tango: When and Where Dual Nutrient (N & P) Reductions Are Needed to Protect Lakes and Downstream Ecosystems. *Environmental Science & Technology*, 50(20), 10805–10813.  
<https://doi.org/10.1021/acs.est.6b02575>
- Pease, L. A., Fausey, N. R., Martin, J. F., & Brown, L. C. (2018). Weather, Landscape, and Management Effects on Nitrate and Soluble Phosphorus Concentrations in Subsurface Drainage in the Western Lake Erie Basin. *Transactions of the ASABE*, 61(1), 223–232.  
<https://doi.org/10.13031/trans.12287>

- Plach, J., Puer, W., Macrae, M., Kompanizare, M., McKague, K., Carlow, R., & Brunke, R. (2019). Agricultural Edge-of-Field Phosphorus Losses in Ontario, Canada: Importance of the Nongrowing Season in Cold Regions. *Journal of Environmental Quality*, 48(4), 813–821. <https://doi.org/10.2134/jeq2018.11.0418>
- Qi, J., Li, S., Li, Q., Xing, Z., Bourque, C. P.-A., & Meng, F.-R. (2016a). A new soil-temperature module for SWAT application in regions with seasonal snow cover. *Journal of Hydrology*, 538, 863–877. <https://doi.org/10.1016/j.jhydrol.2016.05.003>
- Qi, J., Li, S., Li, Q., Xing, Z., Bourque, C. P.-A., & Meng, F.-R. (2016b). Assessing an Enhanced Version of SWAT on Water Quantity and Quality Simulation in Regions with Seasonal Snow Cover. *Water Resources Management*, 30(14), 5021–5037. <https://doi.org/10.1007/s11269-016-1466-8>
- Qi, J., Zhang, X., & Wang, Q. (2019). Improving hydrological simulation in the Upper Mississippi River Basin through enhanced freeze-thaw cycle representation. *Journal of Hydrology*, 571, 605–618. <https://doi.org/10.1016/j.jhydrol.2019.02.020>
- R Core Team (2024). *\_R: A Language and Environment for Statistical Computing\_*. *R Foundation for Statistical Computing, Vienna, Austria*. [Computer software]. <https://www.R-project.org/>
- Schürz, C. (2019). SWATplusR: running SWAT2012 and SWAT+ projects in R. *R package version 0.2*, 7, 1-3.
- Scientific Data Curation Team. (2020). *Metadata record for: Mapping of 30-meter resolution tile-drained croplands using a geospatial modeling approach* [Dataset]. figshare. <https://doi.org/10.6084/M9.FIGSHARE.12668234>
- Scyphers, M. E., Missik, J. E., Kujawa, H., Paulson, J. A., & Bohrer, G. (2024). Bayesian Optimization for Anything (BOA): An open-source framework for accessible, user-friendly Bayesian optimization. *Environmental Modelling & Software*, 182, 106191.

- Shedekar, V. S., Fausey, N. R., King, K. W., & Brown, L. C. (2020). Agricultural drainage: Past, present, and future. *Soil and water conservation: A celebration of*, 75, 140-153.
- Singh, J., H. V. Knapp, and M. Demissie. (2004). Hydrologic modeling of the Iroquois River watershed using HSPF and SWAT. ISWS CR 2004-08. *Champaign, Ill.: Illinois State Water Survey*. [www.sws.uiuc.edu/pubdoc/CR/ISWSCR2004-08.pdf](http://www.sws.uiuc.edu/pubdoc/CR/ISWSCR2004-08.pdf)
- Skaggs, R. W. (1978). DRAINMOD, A water management model for shallow water table soils. *Water Resour. Res. Ins. Of the Univ. Of North Carolina, Report*, (134).
- Skaggs, R. W., Brevé, M. A., & Gilliam, J. W. (1994). Hydrologic and water quality impacts of agricultural drainage\*. *Critical Reviews in Environmental Science and Technology*, 24(1), 1–32. <https://doi.org/10.1080/10643389409388459>
- Smith, D. R., King, K. W., Johnson, L., Francesconi, W., Richards, P., Baker, D., & Sharpley, A. N. (2015). Surface Runoff and Tile Drainage Transport of Phosphorus in the Midwestern United States. *Journal of Environmental Quality*, 44(2), 495–502. <https://doi.org/10.2134/jeq2014.04.0176>
- Stewart, S. (2012). Lake Erie. *Michigan State University Extension*. [https://www.canr.msu.edu/news/lake\\_erie\\_the\\_e\\_in\\_homes#:~:text=The%20Lake%20Erie%20basin%20has.and%20vineyards%20along%20the%20coast](https://www.canr.msu.edu/news/lake_erie_the_e_in_homes#:~:text=The%20Lake%20Erie%20basin%20has.and%20vineyards%20along%20the%20coast).
- SSURGO, Soil Survey Geographic (SSURGO) Database. *Soil Survey Staff, Natural Resources Conservation Service, United States Department of Agriculture*. Date Accessed: January 2024. <https://sdmdataaccess.sc.egov.usda.gov>
- SWAT+ Source Code (Version 61.0.2). (2025). [Computer software]. <https://www.google.com/url?q=https://github.com/swat-model/swatplus&sa=D&source=docs&ust=1763825368938096&usg=AOvVaw2BcoSQA7T4QII0lg5W0k8R>
- SWAT Documentation. (n.d.). Retrieved November 14, 2025, from <https://swat.tamu.edu/docs/>
- SWAT2012 Source Code (Version 692). (2023). [Computer software]. [https://bitbucket.org/blacklandgrasslandmodels/swat\\_development/src/master/](https://bitbucket.org/blacklandgrasslandmodels/swat_development/src/master/)

- The Cadmus Group, (2012). Total Maximum Daily Load and Watershed Management Plan for Total Phosphorus and Total Suspended Solids in the Lower Fox River Basin and Lower Green Bay.
- USDA Natural Resources Conservation Service. (2009, October). *Soil Quality Indicators*. USDA. [https://www.nrcs.usda.gov/sites/default/files/2022-10/total\\_organic\\_carbon.pdf](https://www.nrcs.usda.gov/sites/default/files/2022-10/total_organic_carbon.pdf)
- USGS-NED, 2023. U.S. Geological Survey, National Elevation Dataset, 1/3 Arc-Second. Date Accessed: July 2023. <https://nationalmap.gov/elevation.html>
- Vazquez-AmáBILE, G. G., & Engel, B. A. (2005). Use of SWAT to compute groundwater table depth and streamflow in the Muscatatuck River watershed. *Transactions of the ASAE*, 48(3), 991–1003. <https://doi.org/10.13031/2013.18511>
- Vollmer-Sanders, C., Allman, A., Busdeker, D., Moody, L. B., & Stanley, W. G. (2016). Building partnerships to scale up conservation: 4R Nutrient Stewardship Certification Program in the Lake Erie watershed. *Journal of Great Lakes Research*, 42(6), 1395–1402. <https://doi.org/10.1016/j.jglr.2016.09.004>
- Wang, X., Hollanders, P. H. J., Wang, S., & Fang, S. (2004). Effect of field groundwater table control on water and salinity balance and crop yield in the Qingtongxia Irrigation District, China. *Irrigation and Drainage*, 53(3), 263–275. <https://doi.org/10.1002/ird.117>
- Williams, M. R., King, K. W., & Fausey, N. R. (2015). Contribution of tile drains to basin discharge and nitrogen export in a headwater agricultural watershed. *Agricultural Water Management*, 158, 42–50. <https://doi.org/10.1016/j.agwat.2015.04.009>
- Williams, M. R., King, K. W., Ford, W., & Fausey, N. R. (2016). Edge-of-field research to quantify the impacts of agricultural practices on water quality in Ohio. *Journal of Soil and Water Conservation*, 71(1), 3. <https://doi.org/10.2489/jswc.71.1.9A>
- Xu, X., Huang, G., Sun, C., Pereira, L. S., Ramos, T. B., Huang, Q., & Hao, Y. (2013). Assessing the effects of water table depth on water use, soil salinity and wheat yield: Searching for a target depth for irrigated areas in the upper Yellow River basin. *Agricultural Water Management*, 125, 46–60. <https://doi.org/10.1016/j.agwat.2013.04.004>

- Yang, Q., Benoy, G. A., Chow, T. L., Daigle, J.-L., Bourque, C. P.-A., & Meng, F.-R. (2012). Using the Soil and Water Assessment Tool to Estimate Achievable Water Quality Targets through Implementation of Beneficial Management Practices in an Agricultural Watershed. *Journal of Environmental Quality*, 41(1), 64–72. <https://doi.org/10.2134/jeq2010.0250>
- Yang, Q., Meng, F.-R., Zhao, Z., Chow, T. L., Benoy, G., Rees, H. W., & Bourque, C. P.-A. (2009). Assessing the impacts of flow diversion terraces on stream water and sediment yields at a watershed level using SWAT model. *Agriculture, Ecosystems & Environment*, 132(1–2), 23–31. <https://doi.org/10.1016/j.agee.2009.02.012>
- Yousfi, A., Mechergui, M., & Ritzema, H. (2014). A drain-spacing equation that takes the horizontal flow in the unsaturated zone above the groundwater table into account. *Irrigation and Drainage*, 63(3), 373–382. <https://doi.org/10.1002/ird.1821>
- Zopp, Z. P., Ruark, M. D., Thompson, A. M., Stuntebeck, T. D., Cooley, E., Radatz, A., & Radatz, T. (2019). Effects of Manure and Tillage on Edge-of-Field Phosphorus Loss in Seasonally Frozen Landscapes. *Journal of Environmental Quality*, 48(4), 966–977. <https://doi.org/10.2134/jeq2019.01.0011>

## Appendices

**Appendix 1:** Description of SWAT2005, a previous method for perched water table depth calculation that was not included in the methods of this thesis.

### SWAT2005

The perched water table depth algorithm used in the SWAT2005 method described in Moriasi et al.

(2009), is based on evapotranspiration (ET), precipitation, and surface runoff over a 30-day time period.

$$h = \frac{tdprcp - tdqsur - tdET}{tdET}$$

$$w = \min(0.1, |h|)$$

$$y = \min wtd \quad \text{if } w > 0$$

$$y = \max wtd \quad \text{if } w \leq 0$$

$$wtdpth_t = wtdpth_{t-1} - w * (wtdpth_{t-1} - y)$$

Where  $tdprcp$  is a moving 30-day sum of precipitation,  $tdqsur$  is a moving 30-day sum of surface runoff,  $tdET$  is a moving 30-day sum of ET,  $\min wtd$  is the smallest distance between the surface and water table for the day,  $\max wtd$  is the largest difference between the surface and water table for the day,  $wtdpth_t$  is the depth of the water table at the current time step, and  $wtdpth_{t-1}$  is the depth of the water table at the previous time step.

**Appendix 2:** Description of SWAT-M, a previous method for perched water table depth calculation that inspired aspects of the IWTDN=2 method, but was not included in the methods of this thesis.

### SWAT-M

SWAT-M uses soil moisture above saturation to calculate the perched water table height by layer (Du et al., 2005). SWAT-M inspired aspects of the IWTDN=2 method, but was not included in the methods of this thesis. However, the equations in SWAT-M do not appear to have been integrated into the SWAT source code for SWAT2005, SWAT2009, or SWAT2012 as it was published in Du et al. (2005).

The perched water table depth algorithm shown below is used in the SWAT-M method. It calculates total pore space and routes soil water into the soil layers starting at the impervious layer. First, the impervious layer is set at the bottom of the soil profile. Then starting at the impervious layer, pore spaces within the soil profile are filled with air and water until an unsaturated layer is reached. Then, the water table height above the impervious layer is calculated in the unsaturated layer.

$$por_l = 1 - \frac{bd_l}{2.65}$$

Where  $por_l$  is the total porosity of a certain layer,  $bd_l$  is the bulk density of a certain layer ( $Mg/m^3$ ), and 2.65 is the particle density ( $Mg/m^3$ ).

Saturation is then calculated for each layer of the soil profile.

$$sat_l = fc_l + (por_l - fc_l) * V_{air}$$

Where  $sat_l$  is the saturation of a certain layer (mm),  $fc_l$  is the field capacity of a certain layer (mm),  $por_l$  is the total porosity of a certain layer (mm), and  $V_{air}$  is the pore volume above field capacity filled with air.  $V_{air} = 0.5$  in the Du et al. (2005) example problem.

If the soil water in a layer is greater than saturation plus pore space, excess water is moved to the soil layer above. The water table is set at the top of the saturated layer.

$$sw_{l+1} = sw_{l+1} + (sw_l - sat_l), \quad \text{if } sw_l > sat_l$$

$$wtdpth_t = hght_t, \quad \text{if } sw_l > sat_l$$

Where  $sat_l$  is the saturation of a certain layer (mm),  $sw_l$  is the soil water content of a certain layer (mm),  $sw_{l+1}$  is the soil water content of the soil layer above (mm),  $wtdpth_t$  is the depth of the water table at the current time step (mm), and  $hght_t$  is the height from the impervious layer to the top of the current soil layer (mm).

If the soil water in a layer is not greater than saturation plus pore space, water table is calculated in that layer.

$$wtld_l = \frac{sw_l - fc_l}{(sat_l - fc_l) * V_{air}} * lyrtk_l \text{ if } sw_l \geq sat_l \text{ \& } sw_{l+1} < sat_{l+1}$$

Where  $wtld_l$  is the height from the bottom of the soil layer to the water table (mm),  $sw_l$  is the soil water content of a certain layer (mm),  $fc_l$  is the field capacity of a certain layer (mm),  $sat_l$  is the saturation of a certain layer (mm),  $V_{air}$  is the fraction of pore volume filled with air, and  $lyrtk_l$  is the thickness of the current layer (mm).

Finally, the location of the water table within the unsaturated layer is added to the height of the saturated layers above the impervious layer.

$$wtdpth_t = wtdpth_{t-1} + wtld_l$$

Where  $wtld_l$  is the height from the bottom of the soil layer to the perched water table (mm),  $wtdpth_t$  is the depth of the perched water table from the soil surface at the current time step (mm), and  $wtdpth_{t-1}$  is the depth of the perched water table from the soil surface at the previous time step (mm).

Limitations to the SWAT-M approach are as follows. The SWAT source code (SWAT2005, SWAT2009, and SWAT2012) set  $V_{air} = 0.5$  which creates a very small denominator leading to an unrealistically high water table. Another limitation is that if the perched water table height is calculated to be deeper in the soil profile, but a soil layer is saturated close to the top of the soil profile, the SWAT-M method would not account for a more shallow saturated layer. SWAT-M also sets the impervious layer to the bottom of the soil profile which limits the flexibility of the algorithm to fit different soil profile environments (Du et al., 2005). The Kalcic Lab perched water table calculations aimed to improve on these limitations.

**Appendix 3:** Description of SWAT2009, a previous method for perched water table depth calculation that the Kalcic Lab method took inspiration from, but was not included in the methods of this thesis.

### SWAT2009

The perched water table depth algorithm used in SWAT 2005, SWAT2009, and SWAT2012 ( $IWTDN = 0$ ), is based on the fraction of total soil water in the entire profile above field capacity divided by the available pore space above field capacity (Neitsch et al., 2009). This approach is similar to the SWAT-M approach. However, perched water table depth is not calculated by layer.

$$\frac{spw - spfc}{(spst - spfc)(1 - V_{air})} \times imp$$

Where  $spw$  is the total soil water at the current time step in the whole SWAT soil profile (mm),  $spfc$  is field capacity for the whole SWAT soil profile (mm),  $spst$  is saturation for the whole SWAT soil profile (mm),  $V_{air}$  is the fraction of pore space above field capacity filled with air ( $V_{air}$  is always 0.5), and  $imp$  is the depth to the impervious layer from the soil surface (mm).

However, in the SWAT2005, SWAT2009, and SWAT2012 source code version 664, more adjustments were made to the equation than are represented in the SWAT2009 documentation (Neitsch et al., 2009). First, there was a bug in the source code where only  $spst$  is multiplied by  $V_{air}$  and  $spfc$  is not. Second, there was an equation added to the source code that is activated when field capacity and saturation are too close together.

$$if\ spst \times V_{air} < 1.1 \times spfc$$

$$spst \times V_{air} = 1.1 \times spfc$$

Since  $V_{air}$  is always equal to 0.5, it is difficult for a model with silt loam soils to have a difference in field capacity and saturation that is large enough for half of saturation to be larger than  $1.1 \times spfc$ . The addition of this equation deviates from the physically based calculation represented in the literature (Neitsch et al., 2009). For these reasons, the SWAT2009 source code is not tested in this thesis.

The Kalcic Lab method for perched water table calculation takes inspiration from the use of soil water, field capacity, and saturation in this method. However, the Kalcic Lab method takes into account the soil profile layers and has not integrated  $V_{air}$ . Future work that includes  $V_{air}$  should consider a smaller or adjustable  $V_{air}$  fraction to avoid a perched water table above the soil surface.

**Appendix 4:** Description of Modified DRAINMOD approach, a previous method for perched water table depth calculation.

#### Modified DRAINMOD approach

The perched water table depth algorithm used beginning in SWAT 2009, titled the modified DRAINMOD approach (Moriasi et al., 2009), is based on the drainage volume in the soil profile multiplied by a water table depth adjustment factor. This approach is the previous version of IWTDN=1 in SWAT2009. The water table depth adjustment factor is a parameter that is calibrated during model calibration. This method was revised in Moriasi et al. (2011) for SWAT2009, because it is difficult to have a single ideal calibration value for water table depth factor for the entire watershed area due to differences in field characteristics.

In the modified DRAINMOD approach, the impervious layer is set equal to the deepest depth of the SWAT soil profile. Drainage volume is computed assuming water enters the area above the impervious layer through infiltration and exits through tile drains, ET, lateral flow, seepage through the impervious layer, and entering nearby streams through shallow aquifers.

$$if\ drvol \geq 0$$

$$drvol = drvol_i - inft + perc + qtile + qlat + ET + qgw + aqrmv$$

$$if\ drvol \leq 0$$

$$drvol = 0$$

Where  $drvol$  is the HRU drainage volume (mm);  $drvol_i$  is the HRU drainage volume at the initiation of the model run ( $drvol_i = 0$ , if unknown)(mm);  $inft$  is the daily infiltration;  $perc$  is the daily deep seepage out of the deepest layer of the soil profile (mm);  $qtile$  is the daily flow out of the tile drains (mm);  $qlat$  is the daily lateral flow (mm);  $ET$  is the daily ET (mm);  $qgw$  is the daily amount of water that moves from shallow aquifers to nearby streams (mm); and  $aq\ rmv$  is the water that leaves the shallow aquifer each month (mm). When all of the pore space is saturated,  $drvol = 0$ .

Drainage volume is used to calculate water table depth using a water table adjustment factor that is calibrated.

$$wtdpth = wtfctr * drvol, \quad \text{if } wtdpth \leq imp$$

$$wtdpth = imp, \quad \text{if } wtdpth > imp$$

Where  $wtdpth$  is the depth of the perched water table (mm);  $drvol$  is the HRU drainage volume;  $wtfctr$  is a calibrated water table factor that will adjust soil water; and  $imp$  is the depth to the impervious layer from the soil surface.

**Appendix 5:** Source code modifications to SWATrunR. On line 212 of the `swat2012_parameter_read.R` file within the SWATrunR source code was modified to handle reading the `output.sol` file.

```

par_list <- map(files, ~ gsub(".*\\:", "", .x[4:6]) %>% as.numeric()) %>%
  map(~ as_tibble(t(.))) %>% ## jaya hafner 3/14/25
  reduce(., rbind) %>%
  set_colnames(., c("SOL_ZMX", "ANION_EXCL", "SOL_CRK")) %>%
  as_tibble(.) %>%
  mutate(., file_code = file_sel$file_code)

```



**Appendix 8:** The model was not calibrated using Nash Sutcliffe Efficiency (NSE). Model calibration was assessed using NSE over the calibration and validation periods. Moriasi et al. (2015) concludes that NSE values of 0.5 and greater for tile flow are satisfactory for the watershed scale at a daily time step and values of 0.4 and greater are satisfactory for a daily timestep at the watershed scale in DRAINMOD. Moriasi et al. (2007b) concludes that values 0.65 and greater are satisfactory for soil volumetric water content and soil temperature for the watershed scale at a monthly time step. Field scale model recommendations for a daily timestep have not been set.

NSE	Calibration Period				Validation Period				Satisfactory NSE
	IWTDN =1	IWTDN =1 & SWAT-FT	IWTDN =2	IWTDN =2 & SWAT-FT	IWTD N=1	IWTD N=1 & SWAT-FT	IWTD N=2	IWTD N=2 & SWAT-FT	
Tmp (°C) at 100 mm	0.8736	0.9540	0.8741	0.9538	0.8793	0.9237	0.8808	0.9137	> 0.65
Tmp (°C) at 200 mm	0.9093	0.9586	0.9101	0.9600	0.9073	0.9351	0.9102	0.9259	> 0.65
Tmp (°C) at 500 mm	0.8901	0.9224	0.8862	0.9257	0.8784	0.9193	0.8752	0.9132	> 0.65
Tile flow (mm)	0.0137	-0.1362	-0.0018	0.0997	-0.1816	-0.1698	-0.1148	0.0247	> 0.50
Water table (mm)	-0.1287	0.1816	-0.0772	0.1029					> 0.40
VWC at 100 mm (mm/mm)	0.0514	0.1013	-0.0248	0.1391	0.1311	0.4848	0.2853	0.3645	> 0.65
VWC at 200 mm (mm/mm)	-5.7845	-1.6429	-0.0247	0.0041	-9.8372	-7.2185	-7.3416	-2.8813	> 0.65
VWC at 500 mm (mm/mm)	0.6075	0.5384	-0.5097	-0.6248	-3.7091	-2.4241	0.1453	-0.4257	> 0.65

**Appendix 9:** The model was not calibrated using  $R^2$ . Model calibration was assessed using  $R^2$  over the calibration and validation periods. Moriasi et al. (2015) estimates that an  $R^2$  greater than 0.6 is satisfactory for daily watershed-scale models, and greater than 0.7 is satisfactory for monthly single-field models. Field scale model recommendations for a daily timestep have not been set.

$R^2$	Calibration				Validation				Satisfactory $R^2$
	IWTDN =1	IWTDN =1 & SWAT-FT	IWTDN =2	IWTDN =2 & SWAT-FT	IWTD N=1	IWTD N=1 & SWAT-FT	IWTD N=2	IWTD N=2 & SWAT-FT	
Tmp (°C) at 100 mm	0.9468	0.9562	0.9466	0.9549	0.9491	0.9279	0.9492	0.9212	> 0.6
Tmp (°C) at 200 mm	0.9734	0.9631	0.9731	0.9628	0.9714	0.9371	0.9719	0.9308	> 0.6
Tmp (°C) at 500 mm	0.9647	0.9346	0.9638	0.9363	0.9713	0.9202	0.9734	0.9162	> 0.6
Tile flow (mm)	0.1183	0.1524	0.0580	0.1360	NA (constant 0 value)	0.0013	0.0504	0.0940	> 0.6
Water table (mm)	0.2267	0.4163	0.2321	0.6374					> 0.6
VWC at 100 mm (mm/mm)	0.2818	0.3566	0.2811	0.3327	0.3871	0.5755	0.6221	0.5861	> 0.6
VWC at 200 mm (mm/mm)	0.1614	0.4469	0.4271	0.4813	0.3919	0.5579	0.4269	0.5301	> 0.6
VWC at 500 mm (mm/mm)	0.6962	0.7395	0.1858	0.1711	0.2493	0.3664	0.3559	0.2636	> 0.6

**Appendix 10:** The model was not calibrated using PBIAS. Model calibration was assessed using PBIAS over the calibration and validation periods. Moriasi et al. (2007b) estimates that A PBIAS of +/- 25% is satisfactory for streamflow at a monthly time step. Field scale model recommendations for a daily timestep have not been set.

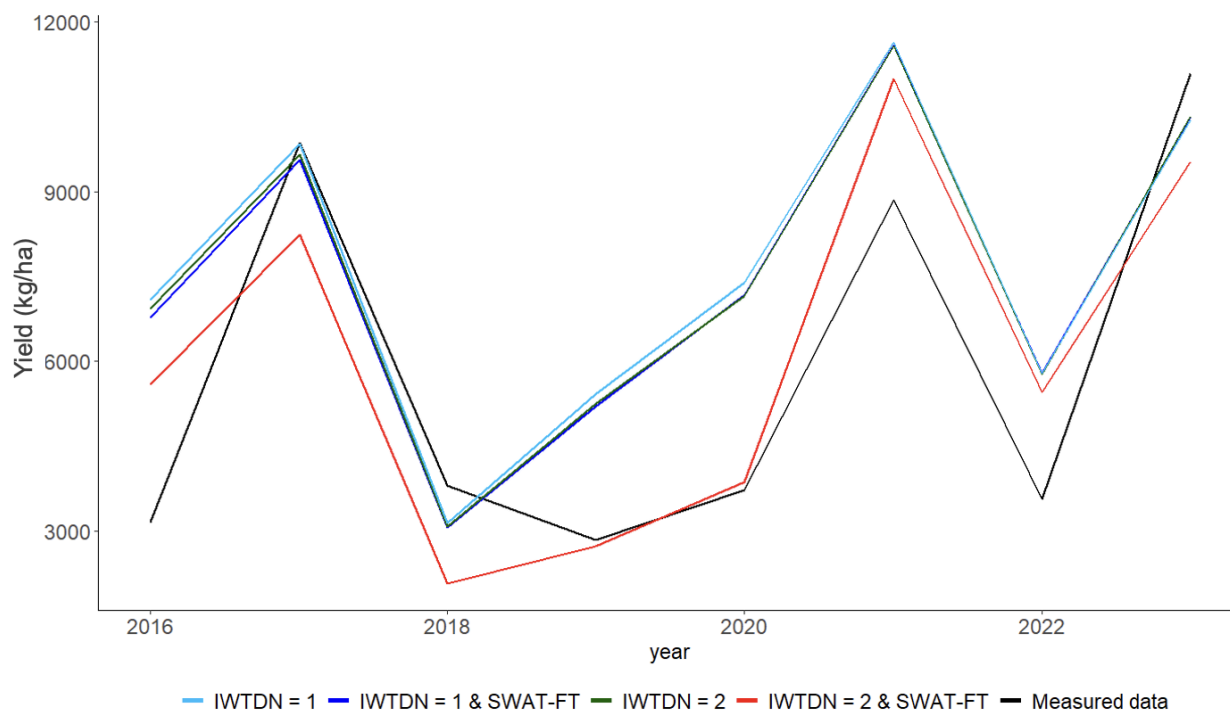
PBIAS	Calibration				Validation				Satisfactory PBIAS
	IWTDN =1	IWTDN =1 & SWAT-FT	IWTDN =2	IWTDN =2 & SWAT-FT	IWTD N=1	IWTD N=1 & SWAT-FT	IWTD N=2	IWTD N=2 & SWAT-FT	
Tmp (°C) at 100 mm	-13.9	-1.0	-13.9	-0.7	-14.5	-1.7	-14.5	-1.5	+/- 25%
Tmp (°C) at 200 mm	-13.2	-0.4	-13.3	-0.1	-13.7	-0.4	-13.7	-0.2	+/- 25%
Tmp (°C) at 500 mm	-13.9	-0.7	-14.0	-0.4	-14.8	0.8	-14.9	1.3	+/- 25%
Tile flow (mm)	-80.3	-13.4	-54.7	-24.9	-100.0	-95.9	-91.8	-61.1	+/- 25%
Water table (mm)	-36.3	-24.9	29.6	26.6					+/- 25%
VWC at 100 mm (mm/mm)	13.4	16.1	9.8	10.6	-13.2	-5.3	-14.0	-10.6	+/- 25%
VWC at 200 mm (mm/mm)	-20.8	-11.1	-4.8	-2.1	-30.3	-24.1	-21.9	-14.1	+/- 25%
VWC at 500 mm (mm/mm)	-0.4	-2.7	15.1	16.0	-17.2	-12.0	4.5	8.4	+/- 25%

**Appendix 11:** The model was not calibrated using KGE. Model calibration was assessed using KGE over the calibration and validation periods. Satisfactory KGE is greater than -0.41 according to Knoben et al. (2019) for hydrology variables. Field scale model recommendations for a daily timestep have not been set for each output variable.

KGE	Calibration				Validation				Satisfactory KGE
	IWTDN =1	IWTDN =1 & SWAT-FT	IWTDN =2	IWTDN =2 & SWAT-FT	IWTD N=1	IWTD N=1 & SWAT-FT	IWTD N=2	IWTD N=2 & SWAT-FT	
Tmp (°C) at 100 mm	0.8072	0.9675	0.8094	0.9746	0.8294	0.8957	0.8330	0.8692	> -0.41
Tmp (°C) at 200 mm	0.8280	0.9487	0.8321	0.9610	0.8430	0.9176	0.8497	0.8892	> -0.41
Tmp (°C) at 500 mm	0.8487	0.9163	0.8397	0.9222	0.8409	0.9213	0.8240	0.8985	> -0.41
Tile flow (mm)	-0.2493	0.3712	-0.1388	0.1751	NA (constant 0 value)	-0.6300	-0.4931	-0.1795	> -0.41
Water table (mm)	0.0907	0.2380	-0.0038	0.1380					> -0.41
VWC at 100 mm (mm/mm)	0.4803	0.5237	0.5201	0.5517	0.5847	0.7527	0.7060	0.7292	> -0.41
VWC at 200 mm (mm/mm)	-0.3639	0.1101	0.1444	0.5233	-0.3624	-0.5314	-0.6649	-0.1043	> -0.41
VWC at 500 mm (mm/mm)	0.7886	0.6821	0.0549	-0.0160	0.1596	0.0693	0.5285	0.1063	> -0.41

**Appendix 12:** Yield results for each executable.

Year	Crop	Field data yield (kg/ha)	SWAT yield IWTDN=1 (kg/ha)	SWAT yield IWTDN=1 & SWAT-FT (kg/ha)	SWAT yield IWTDN=2 (kg/ha)	SWAT yield IWTDN=2 & SWAT-FT (kg/ha)
2016	Soy	3159.452	7089.06	6784.76	6940.42	5596.37
2017	Corn	9865.1837	9852.13	9558.09	9654.52	8234.61
2018	Soy	3803.0441	3136.80	3068.14	3074.88	2073.30
2019	Soy	2837.656	5421.36	5207.05	5258.51	2730.43
2020	Soy	3720.5472	7385.61	7177.91	7155.29	3863.33
2021	Corn	8857.4499	11640.92	11587.16	11582.10	10989.08
2022	Soy	3569.0106	5793.54	5806.48	5776.75	5447.53
2023	Corn	11085.072	10277.62	10314.99	10331.29	9537.97

**Appendix 13:** Time series plot of the yield results for each executable compared to measured data from the field.

RSR,  $R^2$ , and PBIAS results show that the *IWTDN=2 & SWAT-FT* executable produced the yield outputs that most closely matched measured data (Appendix 12-14). We have found that this was likely an artifact of the random set of parameters chosen in calibration of the *IWTDN=2 & SWAT-FT* model. There are other more robust findings for *IWTDN=2 & SWAT-FT* improvements.

**Appendix 14:** Statistics comparing yield results for each executable to measured data.

Statistic	IWTDN=2 & SWAT-FT (kg/ha)	IWTDN=1 & SWAT-FT (kg/ha)	IWTDN=2 (kg/ha)	IWTDN=1 (kg/ha)
RSR	0.5127	0.8240	0.8324	0.8718
$R^2$	0.7434	0.7039	0.7021	0.6875
PBIAS	-3.2	-21.2	-21.5	-22.6